



# Spatiotemporal Variability in the Oxidative Potential of Ambient Fine Particulate Matter in Midwestern United States

Haoran Yu<sup>1</sup>, Joseph Varghese Puthussery<sup>1</sup>, Yixiang Wang<sup>1</sup>, Vishal Verma<sup>1\*</sup>

<sup>1</sup>Department of Civil and Environmental Engineering, University of Illinois at Urbana-Champaign, Urbana, IL, 61801, United States

\* Correspondence to: Vishal Verma (vverma@illinois.edu)

**Abstract.** We assessed the oxidative potential (OP) of both water-soluble and methanol-soluble fractions of ambient fine particulate matter (PM<sub>2.5</sub>) in the midwestern United States. A large set of PM<sub>2.5</sub> samples (N = 241) were collected from five sites, setup in different environments, i.e. urban, rural and roadside, in Illinois, Indiana and Missouri during May 2018 – May 2019. Five acellular OP endpoints, including the consumption rate of ascorbic acid and glutathione in a surrogate lung fluid (SLF) (OP<sup>AA</sup> and OP<sup>GSH</sup>, respectively), dithiothreitol (DTT) depletion rate (OP<sup>DTT</sup>), and ·OH generation rate in SLF and DTT (OP<sup>OH-SLF</sup> and OP<sup>OH-DTT</sup>, respectively), were measured for all PM<sub>2.5</sub> samples. PM<sub>2.5</sub> mass concentrations in the Midwest US as obtained from these samples were spatially homogeneously distributed, while most OP endpoints showed significant spatiotemporal heterogeneity. Seasonally, higher activities occurred in summer for most OP endpoints for both water- and methanol-soluble extracts. Spatially, roadside site showed highest activities for most OP endpoints in the water-soluble extracts, while only occasional peaks were observed at urban sites in the methanol-soluble OP. Most OP endpoints showed similar spatiotemporal trends between mass- and volume-normalized activities across different sites and seasons. Comparisons between two solvents (i.e. water and methanol) showed that methanol-soluble OP generally had higher activity levels than corresponding water-soluble OP. Site-to-site comparisons of OP showed stronger correlations for methanol-soluble OP compared to water-soluble OP, indicating a better extraction of water-insoluble redox-active compounds from various emission sources into methanol. We found a weak correlation and inconsistent slope values between PM<sub>2.5</sub> mass and most OP endpoints. Moreover, the poor-to-moderate intercorrelations among different OP endpoints infer different mechanisms of OP represented by these endpoints, and thus demonstrate the rationale for analyzing multiple acellular endpoints for a better and comprehensive assessment of OP.

## 1 Introduction

Oxidative stress induced by ambient fine particulate matter (PM<sub>2.5</sub>; particulate matter with size less than 2.5 µm) has been widely recognized as a biological pathway for fine particles to exert adverse health effect in humans (Sørensen et al., 2003; Risom et al., 2005; Garçon et al., 2006; Wessels et al., 2010; Cachon et al., 2014; Haberzettl et al., 2016; Feng et al., 2016; Rao et al., 2018; Mudway et al., 2020). A variety of chemical species in ambient particles, such as transition metals and aromatic organic species, possess redox cycling capability and can catalyze electron transfer from cellular reductants (e.g. NADPH) to molecular oxygen (O<sub>2</sub>), which subsequently forms highly reactive radicals [e.g. superoxide radical (·O<sub>2</sub><sup>-</sup>) and hydroxyl radical (·OH)] and non-radical oxidants [e.g. hydrogen peroxide (H<sub>2</sub>O<sub>2</sub>)].



34 (Kampfrath et al., 2011;Qin et al., 2018;Kumagai et al., 2002;Lee et al., 2016). These oxygen containing species with  
35 high redox activity and short lifetime are collectively defined as the reactive oxygen species (ROS). Several  
36 antioxidants (e.g. ascorbic acid (AA), reduced glutathione (GSH) and uric acid (UA) etc.) that are present in human  
37 respiratory tract lining fluid (RTLFL) can counteract the ROS under normal conditions by donating extra electrons, thus  
38 forming less-oxidative species and oxidized antioxidants (Kelly, 2003;Li and Nel, 2006;Allan et al., 2010;Zuo et al.,  
39 2013;Poljšak and Fink, 2014). However, excessively produced ROS might penetrate the antioxidant barrier and induce  
40 oxidative stress (Xing et al., 2016;Rao et al., 2018), leading to the cascade of detrimental biological effects such as  
41 oxidation of DNA, lipids and proteins (Rossner et al., 2008;Franco et al., 2008;Grevendonk et al., 2016), tissue injury  
42 (Feng et al., 2016;Gurgueira et al., 2002;Sun et al., 2020) and eventually cardiopulmonary impairment (Li et al.,  
43 2018;Kodavanti et al., 2000;Kampfrath et al., 2011). The capability of particulate matter (PM) for catalyzing the  
44 generation of ROS and/or the depletion of antioxidants is defined as the oxidative potential (OP) of PM (Bates et al.,  
45 2019).

46 The assessment of PM<sub>2.5</sub>-induced oxidative stress is conventionally carried out through biological tests, including both  
47 *in vitro* (Becker et al., 2005;Zhang et al., 2008;Oh et al., 2011;Yan et al., 2016;Abbas et al., 2016;Deng et al., 2013)  
48 and *in vivo* designs (Kleinman et al., 2005;Riva et al., 2011;Pei et al., 2016;Araujo et al., 2008;Xu et al., 2011;Sancini  
49 et al., 2014). Although, these biological tests are highly relevant in terms of representing the health effects in humans,  
50 the time- and labor-intensive protocols as well as the cost of experimental materials generally limit their application  
51 to only small sample sizes. Various acellular chemical assays which assess the OP by replicating intrinsic biological  
52 mechanisms were therefore developed as alternatives. These assays are generally divided in two categories. The OP  
53 analysis approaches in the 1<sup>st</sup> category directly probe the generation of ROS during redox cycling reactions in presence  
54 of PM, such as the measurement of H<sub>2</sub>O<sub>2</sub> and ·OH production in surrogate lung fluid (SLF) (Vidrio et al., 2009;Shen  
55 et al., 2011;Charrier et al., 2014;Ma et al., 2015), and H<sub>2</sub>O<sub>2</sub> and ·OH production in dithiothreitol (DTT) (Yu et al.,  
56 2018;Xiong et al., 2017;Chung et al., 2006;Kumagai et al., 2002). The assays in 2<sup>nd</sup> category utilize the consumption  
57 of antioxidants such as AA (Visentin et al., 2016;Weichenthal et al., 2016b) and GSH (Künzli et al., 2006;Szigeti et  
58 al., 2016), or surrogates of cellular reductants such as DTT (Verma et al., 2014;Cho et al., 2005), as the OP indicator.  
59 Analyzing each PM sample for all of these chemical assays is also time-consuming. To address this concern, we have  
60 previously developed an automated OP analysis instrument named SAMERA – Semi-Automated Multi-Endpoint  
61 ROS-activity Analyzer, which can measure five most commonly used OP endpoints (i.e. consumption rate of AA and  
62 GSH in SLF, OP<sup>AA</sup> and OP<sup>GSH</sup> respectively; consumption rate of DTT, OP<sup>DTT</sup>, and generation rate of ·OH in SLF and  
63 DTT, OP<sup>OH-SLF</sup> and OP<sup>OH-DTT</sup>) for a PM extract in less than 3 hours (Yu et al., 2020). These acellular endpoints have  
64 been widely implemented by various researchers for assessing the oxidative properties of PM<sub>2.5</sub>. However, there has  
65 not been a single study which has systematically compared the responses of all of these chemical assays in a single  
66 investigation.

67 Although OP is proposed as an integrative PM<sub>2.5</sub> property, purportedly combining the individual and synergistic  
68 actions of its many active components, there have been limited attempts to integrate it in the large-scale  
69 epidemiological studies. This is because, unlike other PM properties such as mass, sulfate, nitrate etc., the OP





measurements in different geographical regions have been relatively sparse. Moreover, before integrating OP in the epidemiological studies, it is important that we investigate the differences of its spatiotemporal distribution with other commonly measured PM properties such as mass. An understanding of the temporal variation of OP in a specific environment could be helpful in time series studies of short-term effects, while the spatial variation of OP can aid in studying the long-term health effects of  $PM_{2.5}$  exposure among different regions (Yang et al., 2015a). Globally, the spatiotemporal profiles of OP have been characterized for some geographical regions such as Los Angeles Basin (Saffari et al., 2014, 2013), Denver (Zhang et al., 2008), Atlanta (Fang et al., 2016; Verma et al., 2014) in US, Ontario (Canada) (Jeong et al., 2020; Weichenthal et al., 2019; Weichenthal et al., 2016a), Netherland (Yang et al., 2015a; Yang et al., 2015b), and some coastal cities of Bohai [Jinzhou, Tianjin and Yantai (Liu et al., 2018)] and Beijing (Yu et al., 2019; Liu et al., 2014) in China. Some of these studies have substantially contributed in enhancing our understanding of the role of OP in the PM-induced health effects (Fang et al., 2016; Tuet et al., 2016; Abrams et al., 2017; Weichenthal et al., 2016a; Yang et al., 2016; Bates et al., 2015). However, despite including many cities ranked high in terms of the air pollution [e.g. Indianapolis (Rosenthal et al., 2008), Chicago (Dominici et al., 2003), St. Louis (Sarnat et al., 2015), Detroit (Zhou et al., 2011), Cincinnati (Kaufman et al., 2019), and Cleveland (Kumar et al., 2013)], the midwestern region of the United States is an understudied region in terms of assessing the oxidative levels of ambient  $PM_{2.5}$ .

Here, we investigate the detailed spatiotemporal profiles of ambient  $PM_{2.5}$  OP in the midwestern United States. Simultaneous ambient  $PM_{2.5}$  samples were collected from five different sites in the Midwest US. The automated instrument – SAMERA facilitated the measurement of OP on our large bulk of  $PM_{2.5}$  samples ( $N = 241$ ) collected from all the sites, which were extracted in both water and methanol separately. This paper mainly discusses the spatiotemporal distribution of the mass concentration and OP of  $PM_{2.5}$  measured by five different endpoints in the Midwest US. Correlations of OP with PM chemical composition and source apportionment analysis of  $PM_{2.5}$  OP will be presented in our subsequent publications. Our paper presents the results from probably one of the most comprehensive OP analysis campaigns, combining five different acellular OP endpoints measured on both water- and organic-soluble extracts.

## 2 Experimental methods

### 2.1 Sampling campaign

Simultaneous sampling in five different sites spread across three states (i.e. Illinois, Indiana and Missouri) was conducted every week for this project in the Midwest US. The locations of the sampling sites are shown in Figure 1. Champaign (CMP) and Bondville (BON) sites are paired sites representing the urban (roadside) and rural environment of Champaign County, IL, respectively; while three major city sites [i.e. Chicago (CHI), Indianapolis (IND) and St. Louis (STL)] are representatives of urban background regions of Chicago, Indianapolis and St. Louis, respectively. CMP is located on a parking garage in the campus of University of Illinois at Urbana-Champaign, and is adjacent to a 2-lane (both ways) road (i.e. University Avenue). This site is surrounded by the university facilities and is impacted



103 by traffic emissions from adjacent road. The site is about 1 km from downtown Champaign and is surrounded by  
104 dense housing and business development.

105 BON is a rural site, 15 km west of downtown Champaign, and is also a part of the IMPROVE (Interagency Monitoring  
106 of Protected Visual Environments) monitoring program. The station is managed by the Illinois State Water Survey,  
107 and is surrounded by intensively managed agricultural fields. The major highways (I-57 and I-74) are at least 6 km  
108 north and east of this site, respectively.

109 CHI site is located on a dormitory building – Carman hall in Illinois Institute of Technology (IIT) campus, Chicago,  
110 IL. This site is ~500 m away from a two-way 6-lane (including an emergency lane) interstate highway I-90/94, 1.5  
111 km west of Lake Michigan and 5 km south of downtown Chicago. The highway I-90/94 has an annual average daily  
112 traffic flow of 300,000 vehicles per day, and heavy-duty vehicles account for ~10% in the traffic fleet (Xiang et al.,  
113 2019). The site is situated in the mixed commercial and residential area of Chicago, and therefore the emissions from  
114 both traffic mixed with residential and commercial activities are expected.

115 IND site is located inside the campus of School of Public Health, Indiana University – Purdue University Indianapolis  
116 (IUPUI). This site is close to downtown Indianapolis (2 km southeast of IND site) and a two-way 4-lane interstate  
117 highway I-65 (1 km northeast of IND site). The site is surrounded by miscellaneous facilities of IUPUI and Riley  
118 Hospital, therefore the sources of ambient aerosols at IND site may include vehicular emissions from highway, and  
119 emissions from residential and commercial activities related to miscellaneous university and hospital operations.

120 STL site is located 3 km north of downtown St. Louis, MO. This site is 230 m west of the interstate I-44/70 and 1.2  
121 km west of Mississippi River. It is also surrounded by several industries for steel processing, zinc smelting and copper  
122 production (Lee et al., 2006). Therefore, a significant portion of metals in PM at this site is supposed to be from  
123 industrial emissions. The urban activities in downtown St. Louis as well as traffic emissions from highway vehicles  
124 and river boating are also potential sources of PM<sub>2.5</sub> at this site.

125 The sampling period involved four seasons starting from May 22, 2018 to May 30, 2019. Integrated ambient PM<sub>2.5</sub>  
126 samples were collected simultaneously for three continuous days from all the sites. Each site was instrumented with  
127 a High-volume (Hi-Vol) air sampler equipped with PM<sub>2.5</sub> inlet (flow rate = 1.13 m<sup>3</sup>/min; Tisch Environmental; Cleves,  
128 OH). All the samplers were equipped with a timer to enable automatic start of the sampling on each Tuesday 0:00,  
129 and turn-off on each Friday 0:00. After the sampled filters were collected on Friday (before noon), new filters were  
130 loaded in the filter holder to start next run of sampling. We used quartz filters (Pall TissuquartzTM, 8"×10") for  
131 collecting PM<sub>2.5</sub>. The filters were prebaked at 550 °C for 24 hours before sampling. Total 241 filters were collected  
132 during the whole campaign (44 from CHI, 47 from STL, 54 from IND, 51 from CMP and 45 from BON). We also  
133 collected field blank filters (N = 10 from each site) once in every five weeks by placing a blank quartz filter in filter  
134 holder of the sampler for 1 hour but without running the pump.

135 All filters were weighed before and after sampling using a lab-scale digital balance (0.2 mg readability, Sartorius  
136 A120S, Göttingen, Germany) for determining the PM<sub>2.5</sub> mass loading on each filter. Prior to each weighing, filters  
137 were equilibrated in a constant temperature (24 °C) and relative humidity (50 %) room for 24 hours. After sampling,



the filters were individually wrapped in prebaked (550 °C) aluminum foils and stored in a freezer at -20 °C before analysis. More information on sampling including the exact dates of sampling are provided in Table S1 in the supplemental information (SI).

## 2.2 Sample extraction protocol

Sample extraction protocol for OP analysis was determined by the requirement to keep a relatively constant concentration of PM<sub>2.5</sub> in the liquid extracts. This is due to non-linear response of certain OP endpoints with PM<sub>2.5</sub> mass in the extracts (Charrier et al., 2016). Thus, fraction of the filter and the volume of water used for extraction were varied depending on the PM<sub>2.5</sub> mass loading on each Hi-Vol filter. For the analyses of water-soluble OP, a few (usually 3-5) circular sections (16-25 mm diameter) were punched from the filter and immersed into 15-20 mL of deionized Milli-Q water (DI, resistivity = 18.2 MΩ/cm). The volume of water was adjusted to achieve ~100 µg of total PM<sub>2.5</sub> per mL of DI. The vials containing filter sections suspended in the DI were sonicated in an ultrasonic water bath for 1 hour (Cole-Palmer, Vernon-Hills, IL, US). These suspensions were then filtered through a 0.45 µm PTFE syringe filter to remove all water-insoluble components including filter fibers. 10.5 mL of these filtered extracts were separated and diluted with DI to 15 mL. These diluted extracts were then kept in the sample queue of SAMERA for OP analyses. SAMERA withdraws different volume of these extracts into the reaction vials (RVs) for each OP measurement, i.e. 3.5 mL for OP<sup>AA</sup>, OP<sup>GSH</sup> and OP<sup>OH-SLF</sup>, and 2.1 mL for OP<sup>DTT</sup> and OP<sup>OH-DTT</sup> measurements, all of which were further diluted to 5 mL in the RVs. Thus, the concentrations of PM<sub>2.5</sub> in RVs for SLF-based (i.e. OP<sup>AA</sup>, OP<sup>GSH</sup> and OP<sup>OH-SLF</sup>) and DTT-based (i.e. OP<sup>DTT</sup> and OP<sup>OH-DTT</sup>) assays were maintained constant at 50 µg/mL and 30 µg/mL (±1%), respectively.

For methanol-soluble OP measurements, another fraction from each filter having the same area as used for the water-soluble PM<sub>2.5</sub> extraction was punched and extracted in 10 mL of methanol. After sonication for 1 hour, the suspensions were filtered through 0.45 µm PTFE syringe filter. The filtered extracts were then concentrated to less than 50 µL using a nitrogen dryer to evaporate methanol, and were subsequently reconstituted into 15-20 mL of DI, diluted and analyzed for OP in the same way as water-soluble extracts.

## 2.3 OP analysis

OP activities of PM<sub>2.5</sub> extracts were analyzed using SAMERA. The setup and operation protocol of SAMERA has been discussed in detail in Yu et al. (2020). Briefly, the analysis of all OP endpoints for each extract was conducted in two stages: SLF-based endpoints were analyzed first, while DTT-based assays were conducted in the second stage. For measuring OP<sup>AA</sup> and OP<sup>GSH</sup>, 3.5 mL of the extract was mixed with 0.5 mL SLF and 1 mL of 0.5 M potassium phosphate buffer (K-PB) in an RV. At certain time intervals (i.e. 5, 24, 43, 62 and 81 minutes), two small aliquots of the reaction mixture were withdrawn and dispensed into two measurement vials (MV1 and MV2) separately. The mixture in MV1 was diluted by DI, and was directly injected into a liquid waveguide capillary cell (LWCC-3100; World Precision Instruments, Inc., Sarasota, FL, USA) coupled to an online spectrophotometer (Ocean Optics, Inc., Dunedin, FL, USA), which measured the absorbance at 265 nm (signal from AA) and 600 nm (background) for determining the concentration of AA. 1.6 mL of o-phthalaldehyde (OPA) was added into the reaction mixture



173 contained in MV2 to react with GSH, which forms a fluorescent product. The final mixture in MV2 was then pushed  
174 through a flow cell equipped in a Horiba Fluoromax-4 spectrofluorometer (Horiba Scientific, Edison, NJ, USA), and  
175 the fluorescence was measured at excitation/emission wavelength of 310 nm/427 nm. Simultaneously with the  
176 preparation of the reaction mixture for OP<sup>AA</sup> and OP<sup>GSH</sup> analyses, 3.5 mL of the extract was mixed with 0.5 mL SLF  
177 and 1 mL of 50 mM K-PB buffered disodium terephthalate (TPT) (pH = 7.4) in another RV2. TPT captures ·OH  
178 generated in the reaction and forms another fluorescent product 2-hydroxyterephthalic acid (2-OHTA). Small aliquots  
179 of this reaction mixture were withdrawn into MV2 at selected time intervals (10, 29, 48, 67 and 86 minutes), diluted  
180 by DI, and injected into the flow cell of the spectrofluorometer for measuring fluorescence at the same wavelengths  
181 as used for GSH measurement (i.e. 310 nm excitation/427 nm emission). The concentration of 2-OHTA was  
182 determined by calibrating various concentrations (10-500 nM) of 2-OHTA standards, and the generation rate of ·OH  
183 was determined as the formation rate of 2-OHTA divided by a yield factor (0.35) (Son et al., 2015).

184 Both RVs and MVs were flushed with DI after all SLF-based endpoints were analyzed, and DTT-based assays started  
185 immediately after this cleaning. Similar to the first step of SLF assay, 2.1 mL of the diluted PM<sub>2.5</sub> extract was mixed  
186 with 1 mL of 50 mM TPT, 1.4 mL of DI and 0.5 mL of 1 mM DTT in an RV. At certain time intervals (i.e. 5 min, 17  
187 min, 29 min, 41 min and 53 min), two small aliquots of this reaction mixture were withdrawn and diluted with DI in  
188 MV1 and MV2 separately for the measurement of DTT and ·OH, respectively. DTNB was added into MV1 to capture  
189 residual DTT. The final mixture in MV1 was pushed through LWCC to measure the absorbance at 412 nm, while the  
190 mixture in MV2 was pushed through flow cell of the spectrofluorometer for fluorescence measurement (310 nm  
191 excitation/427 nm emission), respectively. The system was again cleaned by flushing DI to RVs, MVs, LWCC and  
192 flow cell of the spectrofluorometer for the next run. Once in a week, we conducted thorough cleaning of the entire  
193 system, by replacing all chemicals and samples first with methanol followed by DI, and running the program script  
194 10 times with each solvent.

#### 195 2.4 Quality Control/Quality Assurance

196 One field blank filter extract along with a DI blank were used as the negative controls for each set of PM<sub>2.5</sub> samples  
197 analyzed in a batch (usually ~10). Selected metals and organic compounds that are known to be sensitive for different  
198 OP endpoints, i.e. Cu(II) for OP<sup>AA</sup> and OP<sup>GSH</sup>, Fe(II) for OP<sup>OH-SLF</sup>, phenanthraquinone for OP<sup>DTT</sup> and 5-hydroxy-1,4-  
199 naphthoquinone for OP<sup>OH-DTT</sup>, were used as the positive control, and were analyzed weekly with PM<sub>2.5</sub> samples to  
200 ensure the stability of SAMERA and correct for any possible drift.

201 The average and standard deviation of OP of negative and positive controls are shown in Table 1. Our previous study  
202 on the development of SAMERA (Yu et al., 2020) reported the values of OP for negative controls, as  $0.17 \pm 0.07$   
203  $\mu\text{M}/\text{min}$  for OP<sup>AA</sup>,  $0.37 \pm 0.06 \mu\text{M}/\text{min}$  for OP<sup>GSH</sup>,  $4.57 \pm 1.21 \text{ nM}/\text{min}$  for OP<sup>OH-SLF</sup>,  $0.65 \pm 0.02 \mu\text{M}/\text{min}$  for OP<sup>DTT</sup>  
204 and  $-0.38 \pm 0.24 \mu\text{M}/\text{min}$  for OP<sup>OH-DTT</sup>. Consistency of our current results for negative controls with those reported  
205 earlier, and a low coefficient of variation (CoV) obtained for the positive controls (1.1 – 11.8%), ensured a good  
206 quality assurance for the overall OP analysis. We blank corrected all OP values of ambient samples by subtracting the



207 averaged field blank measurements. After blank correction, the OP values below detection limit were replaced with  
 208 half of the detection limits for the corresponding OP endpoint.

## 209 2.5 Statistical analysis

210 To assess spatiotemporal variability in both OP and PM<sub>2.5</sub> mass, we compared their differences among all sites and  
 211 seasons using one-way analysis of variance (ANOVA) test, and different pairs (i.e. pairs of different sites or seasons)  
 212 were compared by Fisher's least significant difference (LSD) post-hoc test. The significant and highly significant  
 213 differences were considered by one-way ANOVA when  $P < 0.05$  and  $P < 0.01$ , respectively. Pearson's correlation  
 214 coefficient ( $r$ ) for single linear regression was computed to determine the correlation of OP between different sites,  
 215 between water-soluble and methanol-soluble OP, between OP and PM<sub>2.5</sub>, as well as the intercorrelation among  
 216 different endpoints for each site. Since several OP endpoints (e.g. OP<sup>AA</sup>, OP<sup>GSH</sup> and OP<sup>DTT</sup>) were abnormally elevated  
 217 in the week of July 4<sup>th</sup> (Independence Day celebration; discussed in section 3.2), we removed this week's sample from  
 218 our regression analysis to avoid any bias caused by this episodic event. Site-to-site comparisons were performed by  
 219 calculating the coefficient of divergence (COD) of mass concentration and volume-normalized OP (i.e. OP<sub>v</sub>) for all  
 220 site pairs, as follows:

$$221 \quad CoD = \sqrt{\frac{1}{N} \sum_{i=1}^N \left( \frac{c_{ij} - c_{ik}}{c_{ij} + c_{ik}} \right)^2}$$

222 where:  $c_{ij}$  and  $c_{ik}$  are the PM<sub>2.5</sub> mass or OP<sub>v</sub> measured in the same week  $i$  at sites  $j$  and  $k$ , respectively;  $N$  is the number  
 223 of the comparable sample pairs for sites  $j$  and  $k$ . COD ranges from 0 to 1. A larger COD (closer to 1) indicates more  
 224 spatial heterogeneity between the sites, while a smaller COD (closer to 0) implies spatial homogeneity. One-way  
 225 ANOVA test was conducted in Matlab R2019a, while other statistical analyses were carried out using Excel.

## 226 3 Results and Discussion

### 227 3.1 PM<sub>2.5</sub> mass concentration

228 Figure 2 shows the time series of three-days averaged PM<sub>2.5</sub> mass concentration at five sampling sites, while the  
 229 seasonal averages are shown in Table 2. The mass concentrations ranged from 2.0 to 21.7 µg/m<sup>3</sup> across all sites, and  
 230 the median was 11.0 µg/m<sup>3</sup>. These results are comparable with previous studies on PM<sub>2.5</sub> in Midwest US cities, e.g.  
 231 St. Louis (3.9 - 48.6 µg/m<sup>3</sup>) (Lee et al., 2006), Chicago (median 9.4 - 10.7 µg/m<sup>3</sup>) (Milando et al., 2016), Detroit (0.6  
 232 - 56.2 µg/m<sup>3</sup>, median 14.4 - 17.6 µg/m<sup>3</sup>) (Gildemeister et al., 2007), Bondville (2.1 - 36.5 µg/m<sup>3</sup>, median 9.5 µg/m<sup>3</sup>)  
 233 and selected cities in Iowa (e.g. Cedar Rapids, Des Moines and Davenport) (8.4 - 11.6 µg/m<sup>3</sup>) (Kundu and Stone,  
 234 2014). Generally, the more urbanized sites of our study (i.e. CHI, STL and IND) showed slightly higher mass  
 235 concentrations (5.7 - 21.7 µg/m<sup>3</sup>) compared to the smaller cities like CMP and its rural component (i.e. BON) (2.0 -  
 236 20.2 µg/m<sup>3</sup>). The highest mass concentrations were recorded at CHI (during winter) and STL (during summer), while  
 237 BON exhibited the lowest concentrations in all seasons, except fall when the mass concentrations were lowest at CMP.



Other than these minor variations, the  $PM_{2.5}$  mass concentrations are both spatially and temporally homogeneous in the Midwest US with no significant seasonal differences.

### 3.2 Time series of $PM_{2.5}$ OP

Time series of both mass- and volume-normalized OP (OP<sub>m</sub> and OP<sub>v</sub>, respectively) at all the sites are shown in Figure 3 (water-soluble OP) and Figure 4 (methanol-soluble OP). Generally, OP for both water- and methanol-soluble extracts showed much more spatiotemporal variability than the  $PM_{2.5}$  mass in the Midwest US. For water-soluble OP, we observed significant spatial variability for SLF-based endpoints (i.e. OP<sup>AA</sup>, OP<sup>GSH</sup> and OP<sup>OH-SLF</sup>) in both mass- and volume-normalized results (Figure 3a-c). CMP showed a substantially higher water-soluble OP than other sites for these endpoints. In the temporal trend, SLF-based endpoints showed higher levels during summer compared to other seasons at most sites. A significant temporal variation was observed for CMP with several spikes in the OP activities throughout the year, most prominently for OP<sup>AA</sup>. The peak in the week of July 3 were observed for multiple endpoints (e.g. OP<sup>AA</sup>, OP<sup>GSH</sup> and OP<sup>DTT</sup>) at most sites, which is attributed to the emissions from firecrackers on Independence Day (July 4) celebrations (Yu et al., 2020; Puthussery et al., 2018). In comparison to SLF-based endpoints, mass- and volume-normalized DTT-based OP (i.e. OP<sup>DTT</sup> and OP<sup>OH-DTT</sup>) showed lesser spatial variations (Figure 3d-e). The spatiotemporal variations for the methanol-soluble OP endpoints (e.g. OP<sup>AA</sup>, OP<sup>GSH</sup>, OP<sup>DTT</sup> and OP<sup>OH-DTT</sup>) seem to be lesser than the corresponding water-soluble OP (Figure 4a-b, d-e). However, methanol-soluble OP<sup>OH-SLF</sup> showed a significant seasonal variability with substantially higher levels in summer at most sites, and a marginal spatial variability with slightly higher activities at CHI during summer (Figure 4c). The spatiotemporal trends for mass- and volume-normalized OP activities were very similar for both water and methanol extracts.

A comparison of the ranges of OP endpoints observed in our study and previous investigations has been briefly provided in SI (Table S2). For water-soluble  $PM_{2.5}$  in our study, OP<sup>AA</sup><sub>m</sub> ranged from 0.002 to 0.077 nmol·min<sup>-1</sup>·μg<sup>-1</sup>, which is within the ranges reported from previous studies conducted in Europe (Künzli et al., 2006; Szigeti et al., 2016; Godri et al., 2011) and India (Mudway et al., 2005). However, our range of OP<sup>AA</sup><sub>v</sub> (0.012 – 0.908 nmol·min<sup>-1</sup>·m<sup>-3</sup>) is much lower than that reported by Fang et al. (2016) (0.2 – 5.2 nmol·min<sup>-1</sup>·m<sup>-3</sup>), probably because of a different protocol used in their study, which involved only AA in the assay. The median of water-soluble OP<sup>GSH</sup><sub>m</sub> (0.007 nmol·min<sup>-1</sup>·μg<sup>-1</sup>) is also comparable with the average of those reported (0.0041 – 0.0083 nmol·min<sup>-1</sup>·μg<sup>-1</sup>) in previous studies (Mudway et al., 2005; Künzli et al., 2006; Godri et al., 2011). Similarly, the median of OP<sup>OH-SLF</sup><sub>m</sub> (0.142 pmol·min<sup>-1</sup>·μg<sup>-1</sup>) is comparable to the averages reported by Vidrio et al. (2009) (0.253 pmol·min<sup>-1</sup>·μg<sup>-1</sup>) and Ma et al. (2015) (0.092 pmol·min<sup>-1</sup>·μg<sup>-1</sup>). The median of OP<sup>DTT</sup><sub>m</sub> (0.014 nmol·min<sup>-1</sup>·μg<sup>-1</sup>) of our samples is significantly lower than the medians or averages reported from most studies conducted in US (0.019 – 0.041 nmol·min<sup>-1</sup>·μg<sup>-1</sup>) (Cho et al., 2005; Charrier and Anastasio, 2012; Gao et al., 2020; Hu et al., 2008; Fang et al., 2015). Similarly, the median of our OP<sup>DTT</sup><sub>v</sub> (0.150 nmol·min<sup>-1</sup>·m<sup>-3</sup>) is lower compared to several studies in Southeast US (0.19 – 0.31 nmol·min<sup>-1</sup>·m<sup>-3</sup>) (Gao et al., 2017; Gao et al., 2020; Fang et al., 2015), but closer to one study conducted in Southwest US (0.14 nmol·min<sup>-1</sup>·m<sup>-3</sup>) (Hu et al., 2008). The range of water-soluble OP<sup>OH-DTT</sup><sub>v</sub> of our samples is quite large (0.004 – 3.565 pmol·min<sup>-1</sup>·m<sup>-3</sup>); however, there is no previous data to compare it, other than reported in the studies conducted by our own group (Xiong et al., 2017; Yu et al., 2018), which were based on a much smaller sample size (N = 10) and limited





spatial extent (single site) and thus resulting into a much narrower range ( $0.2 - 1.1 \text{ pmol} \cdot \text{min}^{-1} \cdot \text{m}^{-3}$ ). Compared to water, only a handful of studies on PM  $\text{OP}^{\text{DTT}}$  used methanol as the PM extraction solvent, while no previous literatures have investigated the OP of PM for other endpoints. The medians of our methanol-soluble  $\text{OP}^{\text{DTT}}_{\text{m}}$  ( $0.021 \text{ nmol} \cdot \text{min}^{-1} \cdot \mu\text{g}^{-1}$ ) and  $\text{OP}^{\text{DTT}}_{\text{v}}$  ( $0.234 \text{ nmol} \cdot \text{min}^{-1} \cdot \text{m}^{-3}$ ) are slightly lower than the medians or averages reported in previous studies in the Southeast US ( $0.027 - 0.034 \text{ nmol} \cdot \text{min}^{-1} \cdot \mu\text{g}^{-1}$  and  $0.28 - 0.30 \text{ nmol} \cdot \text{min}^{-1} \cdot \text{m}^{-3}$ , respectively for  $\text{OP}^{\text{DTT}}_{\text{m}}$  and  $\text{OP}^{\text{DTT}}_{\text{v}}$ ) (Verma et al., 2012; Gao et al., 2017; Gao et al., 2020), which is consistent with the trend for water-soluble  $\text{OP}^{\text{DTT}}$  (i.e. lower levels of our samples than reported previously at other sites).

### 3.3 Spatiotemporal variation in $\text{PM}_{2.5}$ OP

#### *Water-soluble $\text{PM}_{2.5}$ OP*

Seasonally averaged OPm and OPv of water-soluble  $\text{PM}_{2.5}$  at different sites are shown in Figure 5. Differences in both OPm and OPv among different seasons or sites were determined by one-way ANOVA and the results are listed in SI, Table S3. Seasonally, highest OP activities were generally observed in summer, while the lowest activities usually occurred in winter. For example,  $\text{OP}^{\text{AA}}_{\text{v}}$  and  $\text{OP}^{\text{GSH}}_{\text{v}}$  activities had highest levels in summer and lowest levels in winter at CMP and BON, as verified by 1-way ANOVA ( $P < 0.05$ ). Similarly, significantly higher OP activities ( $P < 0.01$  for most cases) were observed for both  $\text{OP}^{\text{OH-SLF}}_{\text{m}}$  and  $\text{OP}^{\text{OH-SLF}}_{\text{v}}$  at all five sites in summer, while winter showed significantly lower levels ( $P < 0.05$ ). For DTT-based endpoints,  $\text{OP}^{\text{OH-DTT}}_{\text{m}}$  and  $\text{OP}^{\text{OH-DTT}}_{\text{v}}$  also showed higher values in summer at CHI, IND and CMP ( $P < 0.01$ ). However,  $\text{OP}^{\text{DTT}}$  exhibited limited temporal variation at most sites with only slightly higher  $\text{OP}^{\text{DTT}}_{\text{m}}$  and  $\text{OP}^{\text{DTT}}_{\text{v}}$  observed in summer at BON ( $P < 0.05$ ). The seasonal trend of mass- and volume-normalized activities were nearly identical for all endpoints, indicating a marginal effect of  $\text{PM}_{2.5}$  mass concentration in the temporal variation of OP.

The temporal variation trend of  $\text{OP}^{\text{DTT}}$  in this study does not correspond with previous studies conducted in Southwest and Southeast US. For the Southeast US, Verma et al. (2014) found significantly higher  $\text{OP}^{\text{DTT}}_{\text{v}}$  in winter (December, 2012) compared to summer (June to August, 2012), and this difference was even more pronounced in mass-normalized OP. Saffari et al. (2014) also observed higher  $\text{OP}^{\text{DTT}}$  activities of quasi-ultrafine particles ( $\text{PM}_{0.25}$ ) in fall and winter seasons for the Southwest US (Los Angeles Basin), and attributed this trend to the partitioning of redox-active semi-volatile organic compounds to particle phase in colder seasons. However, the trend of  $\text{OP}^{\text{AA}}$  in our study is in agreement with another study in Southeast US using  $\text{OP}^{\text{AA}}$  as the endpoint (Fang et al., 2016), which showed higher  $\text{OP}^{\text{AA}}$  in warmer seasons (i.e. summer and fall) than winter. There is no previous literature available on the spatiotemporal trends of other OP endpoints in US, to which we can compare our results.

Spatially, there seems higher variability in the SLF-based endpoints, i.e.  $\text{OP}^{\text{AA}}$  and  $\text{OP}^{\text{GSH}}$  than the DTT-based endpoints ( $\text{OP}^{\text{DTT}}$  and  $\text{OP}^{\text{OH-DTT}}$ ). Highest  $\text{OP}^{\text{AA}}$  and  $\text{OP}^{\text{GSH}}$  activities (both mass- and volume-normalized) occurred at the roadside site CMP (as confirmed by 1-way ANOVA test;  $P < 0.01$ ) in most seasons (except winter for  $\text{OP}^{\text{AA}}_{\text{v}}$ ), while STL and IND had the lowest  $\text{OP}^{\text{AA}}$  and  $\text{OP}^{\text{GSH}}$ .  $\text{OP}^{\text{OH-SLF}}$  was more spatially uniformly distributed than  $\text{OP}^{\text{AA}}$  and  $\text{OP}^{\text{GSH}}$ ; significantly higher  $\text{OP}^{\text{OH-SLF}}_{\text{m}}$  and  $\text{OP}^{\text{OH-SLF}}_{\text{v}}$  were observed at CMP only in summer and spring ( $P < 0.05$ ). For the DTT-based endpoints,  $\text{OP}^{\text{DTT}}_{\text{v}}$  was only marginally higher at CHI in winter, and at CMP in summer





and spring. Other than that, no significant differences were observed for  $OP^{DTT}_v$  among various sites. The spatially uniform pattern for  $OP^{DTT}_v$  is consistent with Verma et al. (2014) which found limited spatial variation for  $OP^{DTT}_v$  in the Southeast US. In contrast, there was significant variation in the  $OP^{DTT}_m$  with elevated levels at CMP ( $P < 0.01$ ) in all seasons. Interestingly, the  $OP^{OH-DTT}$  endpoint showed more spatial variability and was generally lowest at CMP ( $P < 0.05$ ) – the site which showed highest levels for all other OP endpoints. It implies that although  $OP^{DTT}$  and  $OP^{OH-DTT}$  endpoints are measured in the same DTT assay, different chemical components play differential roles in these endpoints. We found very similar spatial patterns of mass- and volume-normalized OP activities for most endpoints, again indicating only a marginal role of  $PM_{2.5}$  mass concentrations in causing the spatial variability in OP levels.

### 3.4 Comparison of water-soluble and methanol-soluble OP

Seasonal averages of methanol-soluble  $PM_{2.5}$  OP<sub>m</sub> and OP<sub>v</sub> are shown in Figure 6. Compared to water-soluble OP, most OP endpoints in the methanol-soluble extracts showed weaker seasonal variations, as also indicated by relatively lower F-values [median of  $F = 1.61$  (Table S4a), compared to 2.71 for the water-soluble OP endpoints (Table S3a)]. Similar to water-soluble OP, highest activities for the methanol-soluble OP were generally observed in summer. For example, highest values of  $OP^{AA}$  and  $OP^{DTT}$  were observed in summer at CMP and BON ( $P < 0.05$ ) for both mass- and volume-normalized activities.  $OP^{OH-SLF}_m$  and  $OP^{OH-SLF}_v$  peaked in summer at BON ( $P < 0.01$ ), but in fall at IND ( $P < 0.05$ ).  $OP^{OH-DTT}_m$  and  $OP^{OH-DTT}_v$  were also elevated in summer at CHI ( $P < 0.01$ ), but showed marginal seasonal variations at other sites. In contrast,  $OP^{GSH}$  showed a rather homogeneous seasonal distribution at all sites, except slight elevation of  $OP^{GSH}_m$  in fall at STL and IND ( $P < 0.05$ ).

The spatial variations in OP were also weaker for the methanol-soluble extracts in comparison to water-soluble extracts [median of  $F = 1.96$  (Table S4b), compared to 4.52 for the water-soluble OP endpoints (Table S3b)]; however, some spikes were observed at certain sites in different seasons. Substantially higher  $OP^{AA}_v$  occurred at CHI ( $P < 0.05$ ) in winter and spring, while no significant differences were observed for  $OP^{AA}_m$  among different sites in any other season.  $OP^{GSH}_v$  was elevated at CHI and CMP during winter and spring ( $P < 0.05$ ), while CMP showed elevated  $OP^{GSH}_m$  in all seasons ( $P < 0.05$ ). In summer and winter,  $OP^{OH-SLF}$  peaked at CHI ( $P < 0.05$ ) for both mass- and volume-normalized levels.  $OP^{OH-DTT}_m$  and  $OP^{OH-DTT}_v$  also peaked at CHI ( $P < 0.05$ ) in summer. The lowest levels of  $OP^{OH-DTT}$  were again found at CMP in all seasons, which is consistent with the trend for water-soluble  $OP^{OH-DTT}$ . In contrast,  $OP^{DTT}$  showed spatially homogeneous distribution across all seasons, with marginally elevated values of  $OP^{DTT}_v$  at STL during fall and winter ( $P < 0.05$ ). The spatiotemporal trends were again very similar between mass- and volume-normalized methanol-soluble OP activities except few cases discussed here.

### 3.4 Comparison of water-soluble and methanol-soluble OP

To assess the effect of solvent on the OP response, we computed the ratio of methanol-soluble OP<sub>v</sub> to water-soluble OP<sub>v</sub> ( $M/W^{OP}$ ) for all samples, and plotted it for the individual sites in Figure 7. As shown in the figure, methanol-soluble extracts generally showed greater response for most of the OP endpoints than the water-soluble extracts, with medians of  $M/W^{OP}$  being either close or greater than 1. The medians for  $M/W^{OP}$  for  $OP^{GSH}_v$  and  $OP^{DTT}_v$  were closer to 1 at many sites (0.6 – 1.3 for  $OP^{GSH}_v$ ; and 1.1 – 1.9 for  $OP^{DTT}_v$ ), while significantly greater than 1 for the other



three endpoints ( $OP^{AA}_v$ ,  $OP^{OH-SLF}_v$  and  $OP^{OH-DTT}_v$ ). The only exception to this trend was for  $OP^{AA}_v$  at CMP, where significantly lower levels of methanol-soluble OP than water-soluble OP were observed (median of  $M/W^{OP} = 0.7$  for  $OP^{AA}_v$  at CMP). Our previous studies analyzing the chemical composition of PM collected at CMP have shown an elevated level of Cu (up to  $60 \text{ ng/m}^3$ ) at this site (Wang et al., 2018; Puthussery et al., 2018), compared to the typical range ( $4 - 20 \text{ ng/m}^3$ ) at most urban sites in US (Buzcu-Guven et al., 2007; Kundu and Stone, 2014; Lee and Hopke, 2006; Hammond et al., 2008; Baumann et al., 2008; Milando et al., 2016). Although water-soluble Cu has been shown as the most important contributor to  $OP^{AA}$  (Fang et al., 2016; Ayres et al., 2008; Visentin et al., 2016), Lin and Yu (2020) reported a strong antagonistic interaction of Cu with imidazole and pyridine, both of which are alkaloid compounds (i.e. reduced organic nitrogen compounds), for oxidizing AA. The unprotonated nitrogen atom in alkaloids tends to chelate Cu, thus reducing its reactivity with AA. Since many of the alkaloid compounds are water-insoluble but methanol-soluble, it is possible that these compounds are efficiently extracted in methanol, causing the apparently lower levels of methanol-soluble  $OP^{AA}$  compared to the water-soluble  $OP^{AA}$  at CMP.

The medians of  $M/W^{OP}$  were very high for both  $\cdot OH$  based endpoints (i.e.  $OP^{OH-SLF}_v$  and  $OP^{OH-DTT}_v$ ) ( $2.1 - 3.8$  for  $OP^{OH-SLF}_v$  and  $1.4 - 1.9$  for  $OP^{OH-DTT}_v$ ), indicating that methanol is able to more efficiently extract the redox-active components driving the response of these OP endpoints. We suspect that one of such components could be organic-complexed Fe. As a Fenton reagent, Fe can catalyze the transfer of electrons from  $H_2O_2$  to  $\cdot OH$  (Held et al., 1996). The generation of  $\cdot OH$  is further enhanced by the complexation of Fe with organic species (Wei et al., 2018; Gonzalez et al., 2017; Xiong et al., 2017; Yu et al., 2018). In a previous study conducted at our CMP site, Wei et al. (2018) found a significant fraction of Fe complexed with hydrophobic organic species ( $28 \pm 22 \%$ ). That study also reported a substantially higher ratio of Fe concentration in 50 % methanol to that in water ( $1.42 \pm 0.19$ ), which showed some seasonality ( $1.97 \pm 0.17$  during winter and  $1.33 \pm 0.20$  in summer). This seasonal pattern of Fe solubility in methanol versus water is consistent with the time series of  $M/W^{OP}$  for  $OP^{OH-SLF}_v$  at most sites (showing higher values in winter than summer; SI Table S5), which further corroborated that Fe complexed with hydrophobic organic fraction of  $PM_{2.5}$  could be majorly responsible for the  $OP^{OH-SLF}_v$  and  $OP^{OH-DTT}_v$  in the methanol extracts. However, detailed chemical characterization will be needed to confirm these hypotheses, which will be explored in our subsequent publications.

We also calculated Pearson's  $r$  for the regression between respective water-soluble and methanol-soluble OP endpoints for individual sites, which are shown in Table 3.  $OP^{DTT}_v$  showed some good correlation between two extraction protocols ( $r = 0.43 - 0.74$  except at STL), while correlations were generally poor ( $r < 0.60$ ) for other four endpoints (i.e.  $OP^{AA}_v$ ,  $OP^{GSH}_v$ ,  $OP^{OH-SLF}_v$  and  $OP^{OH-DTT}_v$ ). It indicates that the components driving the response of  $OP^{DTT}_v$  could be more uniformly extracted in both water and methanol. However, there are additional water-insoluble species driving the response of  $OP^{AA}_v$ ,  $OP^{GSH}_v$ ,  $OP^{OH-SLF}_v$  and  $OP^{OH-DTT}_v$ , which are more efficiently extracted in methanol than water.



### 376 3.5 Site-to-site comparison of OP and mass concentration of $PM_{2.5}$

377 To further evaluate the spatial trend of OP across the Midwest US region, we calculated both COD and correlation  
 378 coefficients (Pearson's  $r$ ) for different site pairs, which are shown in Figure 8 (mass concentrations and water-soluble  
 379 OP of  $PM_{2.5}$ ), and Figure 9 (methanol-soluble  $PM_{2.5}$  OP).

#### 380 *$PM_{2.5}$ mass concentration and water-soluble $PM_{2.5}$ OP*

381  $PM_{2.5}$  mass concentrations showed low levels of COD (0.13 – 0.25, median: 0.20), confirming a spatially  
 382 homogeneous distribution of  $PM_{2.5}$  as indicated earlier (Figure 8a). Conversely, we observed generally higher CODs  
 383 for all water-soluble OPv endpoints, i.e.  $OP^{AA}_v$  (0.38 – 0.56, median: 0.43),  $OP^{GSH}_v$  (0.28 – 0.51, median: 0.35),  
 384  $OP^{OH-SLF}_v$  (0.30 – 0.40, median: 0.35),  $OP^{DTT}_v$  (0.19 – 0.34, median: 0.25), and  $OP^{OH-DTT}_v$  (0.21 – 0.38, median: 0.27)  
 385 (Figure 8b-f). Our results showing a stronger spatial variability in OP than PM mass are largely in agreement with a  
 386 recent study (Daellenbach et al., 2020) analyzing a comprehensive dataset for OP in Europe, which showed that both  
 387 OPv (measured by DTT, 2',7'-Dichlorofluorescein Diacetate and AA assays) and  $PM_{10}$  mass concentrations were  
 388 elevated in the urban environments (e.g. Paris and the Po valley), but  $PM_{10}$  was more regionally distributed than OPv.

389 Interestingly, we found poor correlations for  $PM_{2.5}$  among all site pairs ( $r < 0.60$ ), except IND and BON ( $r = 0.63$ ). It  
 390 implies that despite a homogeneous spatial distribution, emission sources of the chemical species composing  $PM_{2.5}$   
 391 are different at different sites. The correlations were also weak ( $r < 0.60$  for most cases) for the OP endpoints showing  
 392 high CODs, i.e.  $OP^{AA}$ ,  $OP^{GSH}$ ,  $OP^{OH-SLF}$  and  $OP^{OH-DTT}$ , which indicates a more pronounced effect of local point sources  
 393 on these OP endpoints compared to the regional sources. In contrast,  $OP^{DTT}_v$  showed stronger correlation ( $r = 0.48$  –  
 394 0.76, median: 0.62) for most site pairs. Higher correlations for the DTT activity combined with lower CODs suggests  
 395 that the regional sources such as long-range transport or atmospheric processing could have a larger influence on  
 396  $OP^{DTT}$  than the local sources.

#### 397 *Methanol-soluble $PM_{2.5}$ OP*

398 In comparison to water-soluble  $PM_{2.5}$  OP, CODs for the methanol-soluble OP were generally lower (median: 0.21 –  
 399 0.35; Figure 9), indicating higher spatial homogeneity of methanol-soluble PM chemical components that are sensitive  
 400 to OP. Similar to water-soluble  $OP^{DTT}_v$ , the methanol-soluble  $OP^{DTT}_v$  showed the lowest COD (0.14 – 0.26, median:  
 401 0.21) among five endpoints (Figure 9d), which was consistent with Gao et al. (2017) showing a rather low COD (less  
 402 than 0.23) for both water-soluble and methanol-soluble  $OP^{DTT}$  in Southeast US. Overall, higher correlation coefficients  
 403 were observed for the methanol-soluble OP (median: 0.41 – 0.67 for different endpoints) than the corresponding water-  
 404 soluble endpoints (median: 0.13 – 0.62). The correlation coefficients were more elevated for certain endpoints such  
 405 as  $OP^{AA}_v$  ( $r = 0.38$  – 0.62, median: 0.46) and  $OP^{GSH}_v$  ( $r = 0.23$  – 0.65, median: 0.41) than others. It is possible that  
 406 methanol is able to extract more redox-active PM components coming from common emission sources present at these  
 407 sites, and thus yielding to an overall lower spatiotemporal variability and better correlation among different sites.



### 3.6 Correlations of OP with PM<sub>2.5</sub> mass concentration

Pearson's  $r$  and the slope for simple linear regression of volume-normalized OP activities versus PM<sub>2.5</sub> mass concentrations were computed for each individual site, and are listed in Table 4. For both water-soluble and methanol-soluble OP, the endpoints of OP<sup>AA</sup><sub>v</sub>, OP<sup>OH-SLF</sup><sub>v</sub> and OP<sup>OH-DTT</sup><sub>v</sub> were poorly correlated with PM<sub>2.5</sub> mass ( $r < 0.60$  in most cases), while OP<sup>GSH</sup><sub>v</sub> and OP<sup>DTT</sup><sub>v</sub> were moderately-to-strongly correlated with PM<sub>2.5</sub> mass ( $r = 0.38 - 0.73$  for OP<sup>GSH</sup><sub>v</sub>, and  $0.54 - 0.82$  for OP<sup>DTT</sup><sub>v</sub>, except at STL). The lower correlation of OP<sup>AA</sup> and higher correlation of OP<sup>DTT</sup> are consistent with multiple previous studies comparing these endpoints (Visentin et al., 2016; Yang et al., 2014; Janssen et al., 2014). Decent correlations for OP<sup>GSH</sup><sub>v</sub> and OP<sup>DTT</sup><sub>v</sub> showed that PM mass concentrations can drive these endpoints to some extent at few locations. However, it is important to note that despite these good correlations, the slope of regression for OP vs. PM<sub>2.5</sub> mass varied a lot among five sampling sites (range for OP<sup>GSH</sup><sub>v</sub> is  $0.003 - 0.016$  nmol/min/μg, and  $0.005 - 0.028$  nmol/min/μg for OP<sup>DTT</sup><sub>v</sub>), indicating substantial spatiotemporal heterogeneity in the intrinsic potency of the particles to generate ROS at these sites. This is further corroborated by the spatiotemporal variability of OP<sup>GSH</sup><sub>m</sub> and OP<sup>DTT</sup><sub>m</sub> at different sites as shown in Figure 5 and 6. Thus, PM<sub>2.5</sub> mass concentrations have only a limited role in determining the oxidative levels of the PM<sub>2.5</sub> at these sites, and OP seems to be largely driven by the PM chemical composition.

### 3.7 Interrelation among different OP endpoints

We also calculated the correlation coefficient (Pearson's  $r$ ) for all pairs of different OP<sub>v</sub> endpoints at each site, which are listed in Table 5. A high correlation coefficient indicates a common source (or a common pool of chemical components) driving the response of those OP endpoints. For water-soluble OP, the intercorrelations among different endpoints were generally poor at urban sites, i.e. CHI, STL, and IND ( $r < 0.60$ ). Correlations were also poor for nearly all pairs of methanol-soluble OP at STL and IND, but CHI showed significantly elevated  $r$  values among different OP endpoints ( $r = 0.59 - 0.82$ ). Compared to more urbanized sites, the correlations were generally higher at the local sites, i.e. CMP and BON, with  $r > 0.60$  for many pairs of both water-soluble and methanol-soluble OP<sub>v</sub>. Since both of these sites are located in smaller cities, the sources of redox-active components probably have lesser complexity compared to the major city sites, which have multiple and more complex emission sources. For example, CMP is adjacent to a major road, and thus largely impacted by the vehicular emissions. Similarly, BON being a rural site is largely impacted by the agricultural emissions with marginal impact from vehicular emissions and other sources such as long-range transport from surrounding cities (Kim et al., 2005; Buzcu-Guven et al., 2007). Thus, a lack of other major sources contributing to components, which can drive these endpoints in different directions through their interactions (i.e. synergistic or antagonistic), leads to the similarity of their responses and hence a good correlation among them at these two sites. Among all OP endpoints, OP<sup>OH-DTT</sup><sub>v</sub> showed poorest correlations with other endpoints except OP<sup>OH-SLF</sup><sub>v</sub>, with which it was correlated at most sites (i.e. CHI, IND, CMP and BON) for the methanol-soluble extracts ( $r = 0.66 - 0.84$ ). Since both of these endpoints measure the rate of generation of  $\cdot\text{OH}$ , it probably indicates a synergistic role of metals with organic compounds [e.g. Fe with humic-like substances (HULIS), as shown in many previous studies (Yu et al., 2018; Charrier and Anastasio, 2015; Gonzalez et al., 2017; Wei et al., 2018; Ma et al., 2015)] in partly driving



the response of both of these endpoints. Note,  $OP^{OH-DTT}$  is a relatively newly developed assay, and there is hardly any previous literature on its comparison with other OP endpoints.

Overall, a poor-to-moderate and inconstant intercorrelation trend among different endpoints of both water-soluble and methanol-soluble OP at most sites indicates that measuring a single endpoint is not enough to represent the overall OP activity. The diverse range of OP endpoints used in our study could better capture the role of different PM components and their interactions via different pathways for driving the oxidative levels of the PM in a region.

#### 4 Conclusion

We analyzed both water-soluble and methanol-soluble OP of ambient  $PM_{2.5}$  in the Midwest US using five different acellular endpoints, including  $OP^{AA}$ ,  $OP^{GSH}$ ,  $OP^{OH-SLF}$ ,  $OP^{DTT}$  and  $OP^{OH-DTT}$ . The spatiotemporal profiles of all OP endpoints and  $PM_{2.5}$  mass concentration were investigated for one-year timescale from May 2018 to May 2019 using the Hi-Vol filter samples collected from five Midwest US sites located in urban, rural, and roadside environments. Compared to homogeneously distributed  $PM_{2.5}$  mass, all OP endpoints showed significant spatiotemporal variations among different seasons and sites. Seasonally, most OP endpoints generally peaked in summer for both water-soluble and methanol-soluble OP. Spatially, the roadside site showed the highest OP levels for most OP endpoints in water-soluble extracts, while there were occasional peaks in methanol-soluble extracts at other urban sites. Our results showed very limited differences in the spatiotemporal profiles between OPm and OPv for most endpoints, indicating a marginal role of  $PM_{2.5}$  mass in causing the spatiotemporal variability of OP.

Comparing the OP for water- and methanol-soluble extracts, we observed significantly higher OP levels in methanol extracts than the corresponding water-soluble OP activities. This trend was much stronger for  $\cdot OH$  generation endpoints (i.e.  $OP^{OH-SLF}$  and  $OP^{OH-DTT}$ ), indicating a substantial contribution of Fe and its organic complexes, which could be more efficiently extracted in methanol. In comparison to water-soluble OP, methanol-soluble OP showed lower spatial heterogeneity, and higher intercorrelations among different endpoints, which is probably attributed to a more efficient extraction of water-insoluble redox-active species in methanol originated from various emission sources at different sites.

The correlations of OP with  $PM_{2.5}$  mass showed a diverse range, with certain endpoints such as  $OP^{AA}$ ,  $OP^{OH-SLF}$  and  $OP^{OH-DTT}$  showing a poor correlation, while other endpoints (i.e.  $OP^{GSH}$  and  $OP^{DTT}$ ) showing a moderate-to-strong correlation. Despite these occasional strong correlations, the sensitivity of all OP endpoints towards mass, indicated by the slope of OP vs.  $PM_{2.5}$  mass as well as the intrinsic OP (OPm), varied substantially for all OP endpoints across different sites and seasons, showing only a marginal effect of mass concentrations in controlling the oxidative levels of  $PM_{2.5}$ . Moreover, relatively poor and inconsistent correlations among different OP endpoints reflected different pathways of various ROS-active  $PM_{2.5}$  components for exerting oxidative stress.

Collectively, the results obtained through our study provides a strong rationale to recommend that the different endpoints of OP provide useful and additional information than the mass concentrations, which could be relevant to assess the public health impacts associated with ambient  $PM_{2.5}$ . Our future studies will explore the contribution of



different chemical components and their emission sources in determining the oxidative levels of ambient  $PM_{2.5}$  in the Midwest US.

*Data availability.* The data on OP and mass concentration of ambient  $PM_{2.5}$  samples collected in the Midwest US are available upon request from the corresponding author.

*Author contribution.* HY: collection of  $PM_{2.5}$  samples, measurement of OP, data analysis, manuscript organization and writing; JVP: collection of  $PM_{2.5}$  samples, manuscript editing and revision; YW: collection of  $PM_{2.5}$  samples, manuscript editing and revision; VV: conceptualization of study design and methodology, manuscript organization and editing, and overall project supervision.

*Competing Interests.* The authors declare that they do not have any competing interests.

*Acknowledgements.* This material is based upon work supported by the National Science Foundation under Grant No. CBET-1847237. We acknowledge the support from Brent Stephens, Yi Wang, and Will Wetherell for providing us the access to the site in Chicago, Indianapolis and St. Louis, respectively.

## References

- Abbas, I., Verdin, A., Escande, F., Saint-Georges, F., Cazier, F., Mulliez, P., Courcot, D., Shirali, P., Gosset, P., and Garçon, G.: *In vitro* short-term exposure to air pollution  $PM_{2.5-0.3}$  induced cell cycle alterations and genetic instability in a human lung cell coculture model, *Environmental Research*, 147, 146-158, 2016.
- Abrams, J. Y., Weber, R. J., Klein, M., Samat, S. E., Chang, H. H., Strickland, M. J., Verma, V., Fang, T., Bates, J. T., and Mulholland, J. A.: Associations between ambient fine particulate oxidative potential and cardiorespiratory emergency department visits, *Environmental Health Perspectives*, 125, 107008, 10.1289/ehp1545, 2017.
- Allan, K., Kelly, F., and Devereux, G.: Antioxidants and allergic disease: a case of too little or too much?, *Clinical & Experimental Allergy*, 40, 370-380, 2010.
- Araujo, J. A., Barajas, B., Kleinman, M., Wang, X., Bennett, B. J., Gong, K. W., Navab, M., Harkema, J., Sioutas, C., and Lusa, A. J.: Ambient particulate pollutants in the ultrafine range promote early atherosclerosis and systemic oxidative stress, *Circulation Research*, 102, 589-596, 2008.
- Ayres, J. G., Borm, P., Cassee, F. R., Castranova, V., Donaldson, K., Ghio, A., Harrison, R. M., Hider, R., Kelly, F., and Kooter, I. M.: Evaluating the toxicity of airborne particulate matter and nanoparticles by measuring oxidative stress potential—a workshop report and consensus statement, *Inhalation Toxicology*, 20, 75-99, 10.1080/08958370701665517, 2008.
- Bates, J. T., Weber, R. J., Abrams, J., Verma, V., Fang, T., Klein, M., Strickland, M. J., Samat, S. E., Chang, H. H., and Mulholland, J. A.: Reactive oxygen species generation linked to sources of atmospheric particulate matter and cardiorespiratory effects, *Environmental Science & Technology*, 49, 13605-13612, 10.1021/acs.est.5b02967, 2015.
- Bates, J. T., Fang, T., Verma, V., Zeng, L., Weber, R. J., Tolbert, P. E., Abrams, J. Y., Sarnat, S. E., Klein, M., and Mulholland, J. A.: Review of acellular assays of ambient particulate matter oxidative potential: Methods and





- relationships with composition, sources, and health effects, *Environmental Science & Technology*, 53, 4003-4019, 2019.
- Baumann, K., Jayanty, R., and Flanagan, J. B.: Fine particulate matter source apportionment for the chemical speciation trends network site at Birmingham, Alabama, using positive matrix factorization, *Journal of the Air & Waste Management Association*, 58, 27-44, 2008.
- Becker, S., Dailey, L. A., Soukup, J. M., Grambow, S. C., Devlin, R. B., and Huang, Y.-C. T.: Seasonal variations in air pollution particle-induced inflammatory mediator release and oxidative stress, *Environmental Health Perspectives*, 113, 1032-1038, 10.1289/ehp.7996, 2005.
- Buzcu-Guven, B., Brown, S. G., Frankel, A., Hafner, H. R., and Roberts, P. T.: Analysis and apportionment of organic carbon and fine particulate matter sources at multiple sites in the midwestern United States, *Journal of the Air & Waste Management Association*, 57, 606-619, 2007.
- Cachon, B. F., Firmin, S., Verdin, A., Ayi-Fanou, L., Billet, S., Cazier, F., Martin, P. J., Aissi, F., Courcot, D., and Sanni, A.: Proinflammatory effects and oxidative stress within human bronchial epithelial cells exposed to atmospheric particulate matter (PM<sub>2.5</sub> and PM<sub>>2.5</sub>) collected from Cotonou, Benin, *Environmental Pollution*, 185, 340-351, 2014.
- Charrier, J., and Anastasio, C.: On dithiothreitol (DTT) as a measure of oxidative potential for ambient particles: evidence for the importance of soluble transition metals, *Atmospheric Chemistry and Physics*, 12, 11317-11350, 10.5194/acp-12-9321-2012, 2012.
- Charrier, J. G., McFall, A. S., Richards-Henderson, N. K., and Anastasio, C.: Hydrogen peroxide formation in a surrogate lung fluid by transition metals and quinones present in particulate matter, *Environmental Science & Technology*, 48, 7010-7017, 10.1021/es501011w, 2014.
- Charrier, J. G., and Anastasio, C.: Rates of hydroxyl radical production from transition metals and quinones in a surrogate lung fluid, *Environmental Science & Technology*, 49, 9317-9325, 10.1021/acs.est.5b01606, 2015.
- Charrier, J. G., McFall, A. S., Vu, K. K., Baroi, J., Olea, C., Hasson, A., and Anastasio, C.: A bias in the “mass-normalized” DTT response—An effect of non-linear concentration-response curves for copper and manganese, *Atmospheric Environment*, 144, 325-334, 10.1016/j.atmosenv.2016.08.071, 2016.
- Cho, A. K., Sioutas, C., Miguel, A. H., Kumagai, Y., Schmitz, D. A., Singh, M., Eiguren-Fernandez, A., and Froines, J. R.: Redox activity of airborne particulate matter at different sites in the Los Angeles Basin, *Environmental Research*, 99, 40-47, 10.1016/j.envres.2005.01.003, 2005.
- Chung, M. Y., Lazaro, R. A., Lim, D., Jackson, J., Lyon, J., Rendulic, D., and Hasson, A. S.: Aerosol-borne quinones and reactive oxygen species generation by particulate matter extracts, *Environmental Science & Technology*, 40, 4880-4886, 2006.
- Daellenbach, K. R., Uzu, G., Jiang, J., Cassagnes, L.-E., Leni, Z., Vlachou, A., Stefanelli, G., Canonaco, F., Weber, S., and Segers, A.: Sources of particulate-matter air pollution and its oxidative potential in Europe, *Nature*, 587, 414-419, 2020.
- Deng, X., Zhang, F., Rui, W., Long, F., Wang, L., Feng, Z., Chen, D., and Ding, W.: PM<sub>2.5</sub>-induced oxidative stress triggers autophagy in human lung epithelial A549 cells, *Toxicology in vitro*, 27, 1762-1770, 2013.





- 547 Dominici, F., McDermott, A., Zeger, S. L., and Samet, J. M.: Airborne particulate matter and mortality: timescale  
 548 effects in four US cities, *American Journal of Epidemiology*, 157, 1055-1065, 2003.
- 549 Fang, T., Verma, V., Guo, H., King, L. E., Edgerton, E. S., and Weber, R. J.: A semi-automated system for  
 550 quantifying the oxidative potential of ambient particles in aqueous extracts using the dithiothreitol (DTT) assay:  
 551 results from the Southeastern Center for Air Pollution and Epidemiology (SCAPE), *Atmospheric Measurement*  
 552 *Techniques*, 8, 471-482, 10.5194/amt-8-471-2015, 2015.
- 553 Fang, T., Verma, V., Bates, J. T., Abrams, J., Klein, M., Strickland, M. J., Sarnat, S. E., Chang, H. H., Mulholland,  
 554 J. A., and Tolbert, P. E.: Oxidative potential of ambient water-soluble PM<sub>2.5</sub> in the southeastern United States:  
 555 contrasts in sources and health associations between ascorbic acid (AA) and dithiothreitol (DTT) assays,  
 556 *Atmospheric Chemistry and Physics*, 16, 3865-3879, 10.5194/acp-16-3865-2016, 2016.
- 557 Feng, S., Gao, D., Liao, F., Zhou, F., and Wang, X.: The health effects of ambient PM<sub>2.5</sub> and potential mechanisms,  
 558 *Ecotoxicology and Environmental Safety*, 128, 67-74, 10.1016/j.ecoenv.2016.01.030, 2016.
- 559 Franco, R., Schoneveld, O., Georgakilas, A. G., and Panayiotidis, M. I.: Oxidative stress, DNA methylation and  
 560 carcinogenesis, *Cancer Letters*, 266, 6-11, <https://doi.org/10.1016/j.canlet.2008.02.026>, 2008.
- 561 Gao, D., Fang, T., Verma, V., Zeng, L., and Weber, R. J.: A method for measuring total aerosol oxidative potential  
 562 (OP) with the dithiothreitol (DTT) assay and comparisons between an urban and roadside site of water-soluble and  
 563 total OP, *Atmospheric Measurement Techniques*, 10, 2821, 2017.
- 564 Gao, D., Mulholland, J. A., Russell, A. G., and Weber, R. J.: Characterization of water-insoluble oxidative potential  
 565 of PM<sub>2.5</sub> using the dithiothreitol assay, *Atmospheric Environment*, 224, 117327,  
 566 <https://doi.org/10.1016/j.atmosenv.2020.117327>, 2020.
- 567 Garçon, G., Dagher, Z., Zerimech, F., Ledoux, F., Courcot, D., Aboukais, A., Puskaric, E., and Shirali, P.:  
 568 Dunkerque City air pollution particulate matter-induced cytotoxicity, oxidative stress and inflammation in human  
 569 epithelial lung cells (L132) in culture, *Toxicology in vitro*, 20, 519-528, 2006.
- 570 Gildemeister, A. E., Hopke, P. K., and Kim, E.: Sources of fine urban particulate matter in Detroit, MI,  
 571 *Chemosphere*, 69, 1064-1074, <https://doi.org/10.1016/j.chemosphere.2007.04.027>, 2007.
- 572 Godri, K. J., Harrison, R. M., Evans, T., Baker, T., Dunster, C., Mudway, I. S., and Kelly, F. J.: Increased oxidative  
 573 burden associated with traffic component of ambient particulate matter at roadside and urban background schools  
 574 sites in London, *PloS One*, 6, e21961, 10.1371/journal.pone.0021961, 2011.
- 575 Gonzalez, D. H., Cala, C. K., Peng, Q., and Paulson, S. E.: HULIS enhancement of hydroxyl radical formation from  
 576 Fe (II): kinetics of fulvic acid-Fe (II) complexes in the presence of lung antioxidants, *Environmental Science &*  
 577 *Technology*, 51, 7676-7685, 2017.
- 578 Grevendonk, L., Janssen, B. G., Vanpoucke, C., Lefebvre, W., Hoxha, M., Bollati, V., and Nawrot, T. S.:  
 579 Mitochondrial oxidative DNA damage and exposure to particulate air pollution in mother-newborn pairs,  
 580 *Environmental Health*, 15, 1-8, 2016.
- 581 Gurgueira, S. A., Lawrence, J., Coull, B., Murthy, G. K., and González-Flecha, B.: Rapid increases in the steady-  
 582 state concentration of reactive oxygen species in the lungs and heart after particulate air pollution inhalation,  
 583 *Environmental Health Perspectives*, 110, 749-755, 2002.



- 584 Haberzettl, P., O'Toole, T. E., Bhatnagar, A., and Conklin, D. J.: Exposure to fine particulate air pollution causes  
 585 vascular insulin resistance by inducing pulmonary oxidative stress, *Environmental Health Perspectives*, 124, 1830-  
 586 1839, 2016.
- 587 Hammond, D. M., Dvonch, J. T., Keeler, G. J., Parker, E. A., Kamal, A. S., Barres, J. A., Yip, F. Y., and Brakefield-  
 588 Caldwell, W.: Sources of ambient fine particulate matter at two community sites in Detroit, Michigan, *Atmospheric*  
 589 *Environment*, 42, 720-732, 2008.
- 590 Held, K. D., Sylvester, F. C., Hopcia, K. L., and Biaglow, J. E.: Role of Fenton chemistry in thiol-induced toxicity  
 591 and apoptosis, *Radiation Research*, 145, 542-553, 10.2307/3579272, 1996.
- 592 Hu, S., Polidori, A., Arhami, M., Shafer, M., Schauer, J., Cho, A., and Sioutas, C.: Redox activity and chemical  
 593 speciation of size fractioned PM in the communities of the Los Angeles-Long Beach harbor, *Atmospheric Chemistry*  
 594 *and Physics*, 8, 6439-6451, 10.5194/acp-8-6439-2008, 2008.
- 595 Janssen, N. A., Yang, A., Strak, M., Steenhof, M., Hellack, B., Gerlofs-Nijland, M. E., Kuhlbusch, T., Kelly, F.,  
 596 Harrison, R., and Brunekreef, B.: Oxidative potential of particulate matter collected at sites with different source  
 597 characteristics, *Science of the Total Environment*, 472, 572-581, 10.1016/j.scitotenv.2013.11.099, 2014.
- 598 Jeong, C.-H., Traub, A., Huang, A., Hilker, N., Wang, J. M., Herod, D., Dabek-Zlotorzynska, E., Celo, V., and  
 599 Evans, G. J.: Long-term analysis of PM<sub>2.5</sub> from 2004 to 2017 in Toronto: Composition, sources, and oxidative  
 600 potential, *Environmental Pollution*, 263, 114652, 2020.
- 601 Künzli, N., Mudway, I. S., Götschi, T., Shi, T., Kelly, F. J., Cook, S., Burney, P., Forsberg, B., Gauderman, J. W.,  
 602 and Hazenkamp, M. E.: Comparison of oxidative properties, light absorbance, and total and elemental mass  
 603 concentration of ambient PM<sub>2.5</sub> collected at 20 European sites, *Environmental Health Perspectives*, 114, 684-690,  
 604 10.1289/ehp.8584, 2006.
- 605 Kampfrath, T., Maiseyeu, A., Ying, Z., Shah, Z., Deiuliis, J. A., Xu, X., Kherada, N., Brook, R. D., Reddy, K. M.,  
 606 and Padture, N. P.: Chronic fine particulate matter exposure induces systemic vascular dysfunction via NADPH  
 607 oxidase and TLR4 pathways, *Circulation Research*, 108, 716-726, 2011.
- 608 Kaufman, J. A., Wright, J. M., Rice, G., Connolly, N., Bowers, K., and Anixt, J.: Ambient ozone and fine particulate  
 609 matter exposures and autism spectrum disorder in metropolitan Cincinnati, Ohio, *Environmental Research*, 171,  
 610 218-227, <https://doi.org/10.1016/j.envres.2019.01.013>, 2019.
- 611 Kelly, F. J.: Oxidative stress: its role in air pollution and adverse health effects, *Occupational and Environmental*  
 612 *Medicine*, 60, 612-616, 2003.
- 613 Kim, E., Hopke, P. K., Kenski, D. M., and Koerber, M.: Sources of fine particles in a rural midwestern U.S. Area,  
 614 *Environmental Science & Technology*, 39, 4953-4960, 10.1021/es0490774, 2005.
- 615 Kleinman, M. T., Hamade, A., Meacher, D., Oldham, M., Sioutas, C., Chakrabarti, B., Stram, D., Froines, J. R., and  
 616 Cho, A. K.: Inhalation of concentrated ambient particulate matter near a heavily trafficked road stimulates antigen-  
 617 induced airway responses in mice, *Journal of the Air & Waste Management Association*, 55, 1277-1288, 2005.
- 618 Kodavanti, U. P., Schladweiler, M. C., Ledbetter, A. D., Watkinson, W. P., Campen, M. J., Winsett, D. W.,  
 619 Richards, J. R., Crissman, K. M., Hatch, G. E., and Costa, D. L.: The spontaneously hypertensive rat as a model of



- human cardiovascular disease: evidence of exacerbated cardiopulmonary injury and oxidative stress from inhaled emission particulate matter, *Toxicology and Applied Pharmacology*, 164, 250-263, 10.1006/taap.2000.8899, 2000.
- Kumagai, Y., Koide, S., Taguchi, K., Endo, A., Nakai, Y., Yoshikawa, T., and Shimojo, N.: Oxidation of proximal protein sulfhydryls by phenanthraquinone, a component of diesel exhaust particles, *Chemical Research in Toxicology*, 15, 483-489, 2002.
- Kumar, N., Liang, D., Comellas, A., Chu, A. D., and Abrams, T.: Satellite-based PM concentrations and their application to COPD in Cleveland, OH, *Journal of Exposure Science & Environmental Epidemiology*, 23, 637-646, 2013.
- Kundu, S., and Stone, E. A.: Composition and sources of fine particulate matter across urban and rural sites in the Midwestern United States, *Environmental Science: Processes & Impacts*, 16, 1360-1370, 2014.
- Lee, C.-W., Lin, Z.-C., Hu, S. C.-S., Chiang, Y.-C., Hsu, L.-F., Lin, Y.-C., Lee, I. T., Tsai, M.-H., and Fang, J.-Y.: Urban particulate matter down-regulates filaggrin via COX2 expression/PGE2 production leading to skin barrier dysfunction, *Scientific Reports*, 6, 27995, 10.1038/srep27995, 2016.
- Lee, J. H., and Hopke, P. K.: Apportioning sources of PM<sub>2.5</sub> in St. Louis, MO using speciation trends network data, *Atmospheric Environment*, 40, 360-377, 2006.
- Lee, J. H., Hopke, P. K., and Turner, J. R.: Source identification of airborne PM<sub>2.5</sub> at the St. Louis-Midwest Supersite, *Journal of Geophysical Research: Atmospheres*, 111, 2006.
- Li, N., and Nel, A. E.: Role of the Nrf2-mediated signaling pathway as a negative regulator of inflammation: implications for the impact of particulate pollutants on asthma, *Antioxidants & Redox Signaling*, 8, 88-98, 2006.
- Li, Y., Fu, S., Li, E., Sun, X., Xu, H., Meng, Y., Wang, X., Chen, Y., Xie, C., and Geng, S.: Modulation of autophagy in the protective effect of resveratrol on PM<sub>2.5</sub>-induced pulmonary oxidative injury in mice, *Phytotherapy Research*, 32, 2480-2486, 2018.
- Lin, M., and Yu, J. Z.: Assessment of interactions between transition metals and atmospheric organics: ascorbic acid depletion and hydroxyl radical formation in organic-metal mixtures, *Environmental Science & Technology*, 54, 1431-1442, 10.1021/acs.est.9b07478, 2020.
- Liu, Q., Baumgartner, J., Zhang, Y., Liu, Y., Sun, Y., and Zhang, M.: Oxidative potential and inflammatory impacts of source apportioned ambient air pollution in Beijing, *Environmental Science & Technology*, 48, 12920-12929, 2014.
- Liu, W., Xu, Y., Liu, W., Liu, Q., Yu, S., Liu, Y., Wang, X., and Tao, S.: Oxidative potential of ambient PM<sub>2.5</sub> in the coastal cities of the Bohai Sea, northern China: Seasonal variation and source apportionment, *Environmental Pollution*, 236, 514-528, 2018.
- Ma, S., Ren, K., Liu, X., Chen, L., Li, M., Li, X., Yang, J., Huang, B., Zheng, M., and Xu, Z.: Production of hydroxyl radicals from Fe-containing fine particles in Guangzhou, China, *Atmospheric Environment*, 123, 72-78, 10.1016/j.atmosenv.2015.10.057, 2015.
- Milando, C., Huang, L., and Batterman, S.: Trends in PM<sub>2.5</sub> emissions, concentrations and apportionments in Detroit and Chicago, *Atmospheric Environment*, 129, 197-209, 2016.



- 656 Mudway, I., Kelly, F., and Holgate, S.: Oxidative stress in air pollution research, *Free Radical Biology & Medicine*,  
 657 151, 2-6, 10.1016/j.freeradbiomed.2020.04.031, 2020.
- 658 Mudway, I. S., Duggan, S. T., Venkataraman, C., Habib, G., Kelly, F. J., and Grigg, J.: Combustion of dried animal  
 659 dung as biofuel results in the generation of highly redox active fine particulates, *Particle and Fibre Toxicology*, 2, 6,  
 660 10.1186/1743-8977-2-6, 2005.
- 661 Oh, S. M., Kim, H. R., Park, Y. J., Lee, S. Y., and Chung, K. H.: Organic extracts of urban air pollution particulate  
 662 matter (PM<sub>2.5</sub>)-induced genotoxicity and oxidative stress in human lung bronchial epithelial cells (BEAS-2B cells),  
 663 *Mutation Research/Genetic Toxicology and Environmental Mutagenesis*, 723, 142-151,  
 664 <https://doi.org/10.1016/j.mrgentox.2011.04.003>, 2011.
- 665 Pei, Y., Jiang, R., Zou, Y., Wang, Y., Zhang, S., Wang, G., Zhao, J., and Song, W.: Effects of Fine Particulate  
 666 Matter (PM<sub>2.5</sub>) on Systemic Oxidative Stress and Cardiac Function in ApoE<sup>-/-</sup> Mice, *International Journal of*  
 667 *Environmental Research and Public Health*, 13, 484, 2016.
- 668 Poljšak, B., and Fink, R.: The protective role of antioxidants in the defence against ROS/RNS-mediated  
 669 environmental pollution, *Oxidative Medicine and Cellular Longevity*, 2014, 2014.
- 670 Puthussery, J. V., Zhang, C., and Verma, V.: Development and field testing of an online instrument for measuring  
 671 the real-time oxidative potential of ambient particulate matter based on dithiothreitol assay, *Atmospheric*  
 672 *Measurement Techniques*, 11, 5767-5780, 10.5194/amt-11-5767-2018, 2018.
- 673 Qin, G., Xia, J., Zhang, Y., Guo, L., Chen, R., and Sang, N.: Ambient fine particulate matter exposure induces  
 674 reversible cardiac dysfunction and fibrosis in juvenile and older female mice, *Particle and Fibre Toxicology*, 15, 1-  
 675 14, 2018.
- 676 Rao, X., Zhong, J., Brook, R. D., and Rajagopalan, S.: Effect of particulate matter air pollution on cardiovascular  
 677 oxidative stress pathways, *Antioxidants & Redox Signaling*, 28, 797-818, 2018.
- 678 Risom, L., Møller, P., and Loft, S.: Oxidative stress-induced DNA damage by particulate air pollution, *Mutation*  
 679 *Research/Fundamental and Molecular Mechanisms of Mutagenesis*, 592, 119-137, 2005.
- 680 Riva, D. R., Magalhães, C. B., Lopes, A. A., Lanças, T., Mauad, T., Malm, O., Valença, S. S., Saldiva, P. H., Faffe,  
 681 D. S., and Zin, W. A.: Low dose of fine particulate matter (PM<sub>2.5</sub>) can induce acute oxidative stress, inflammation  
 682 and pulmonary impairment in healthy mice, *Inhalation Toxicology*, 23, 257-267, 10.3109/08958378.2011.566290,  
 683 2011.
- 684 Rosenthal, F. S., Carney, J. P., and Olinger, M. L.: Out-of-hospital cardiac arrest and airborne fine particulate  
 685 matter: a case-cross-over analysis of emergency medical services data in Indianapolis, Indiana, *Environmental*  
 686 *Health Perspectives*, 116, 631-636, 2008.
- 687 Rossner, P., Svecova, V., Milcova, A., Lnenickova, Z., Solansky, I., and Sram, R. J.: Seasonal variability of  
 688 oxidative stress markers in city bus drivers: Part II. Oxidative damage to lipids and proteins, *Mutation*  
 689 *Research/Fundamental and Molecular Mechanisms of Mutagenesis*, 642, 21-27,  
 690 <https://doi.org/10.1016/j.mrfmmm.2008.03.004>, 2008.
- 691 Sørensen, M., Daneshvar, B., Hansen, M., Dragsted, L. O., Hertel, O., Knudsen, L., and Loft, S.: Personal PM<sub>2.5</sub>  
 692 exposure and markers of oxidative stress in blood, *Environmental Health Perspectives*, 111, 161-166, 2003.



- 693 Saffari, A., Daher, N., Shafer, M. M., Schauer, J. J., and Sioutas, C.: Seasonal and spatial variation in reactive  
 694 oxygen species activity of quasi-ultrafine particles (PM<sub>0.25</sub>) in the Los Angeles metropolitan area and its association  
 695 with chemical composition, *Atmospheric Environment*, 79, 566-575, 2013.
- 696 Saffari, A., Daher, N., Shafer, M. M., Schauer, J. J., and Sioutas, C.: Seasonal and spatial variation in dithiothreitol  
 697 (DTT) activity of quasi-ultrafine particles in the Los Angeles Basin and its association with chemical species,  
 698 *Journal of Environmental Science and Health, Part A*, 49, 441-451, 10.1080/10934529.2014.854677, 2014.
- 699 Sancini, G., Farina, F., Battaglia, C., Cifola, I., Mangano, E., Mantecca, P., Camatini, M., and Palestini, P.: Health  
 700 risk assessment for air pollutants: alterations in lung and cardiac gene expression in mice exposed to Milano winter  
 701 fine particulate matter (PM<sub>2.5</sub>), *PLoS One*, 9, e109685, 10.1371/journal.pone.0109685, 2014.
- 702 Sarnat, S. E., Winkler, A., Schauer, J. J., Turner, J. R., and Sarnat, J. A.: Fine particulate matter components and  
 703 emergency department visits for cardiovascular and respiratory diseases in the St. Louis, Missouri–Illinois,  
 704 metropolitan area, *Environmental Health Perspectives*, 123, 437-444, 2015.
- 705 Shen, H., Barakat, A., and Anastasio, C.: Generation of hydrogen peroxide from San Joaquin Valley particles in a  
 706 cell-free solution, *Atmospheric Chemistry and Physics*, 11, 753-765, 10.5194/acp-11-753-2011, 2011.
- 707 Son, Y., Mishin, V., Welsh, W., Lu, S.-E., Laskin, J. D., Kipen, H., and Meng, Q.: A novel high-throughput  
 708 approach to measure hydroxyl radicals induced by airborne particulate matter, *International Journal of*  
 709 *Environmental Research and Public Health*, 12, 13678-13695, 10.3390/ijerph121113678, 2015.
- 710 Sun, B., Shi, Y., Li, Y., Jiang, J., Liang, S., Duan, J., and Sun, Z.: Short-term PM<sub>2.5</sub> exposure induces sustained  
 711 pulmonary fibrosis development during post-exposure period in rats, *Journal of Hazardous Materials*, 385, 121566,  
 712 2020.
- 713 Szigeti, T., Dunster, C., Cattaneo, A., Cavallo, D., Spinazzè, A., Saraga, D. E., Sakellaris, I. A., de Kluizenaar, Y.,  
 714 Cornelissen, E. J., and Hänninen, O.: Oxidative potential and chemical composition of PM<sub>2.5</sub> in office buildings  
 715 across Europe–The OFFICAIR study, *Environment International*, 92, 324-333, 10.1016/j.envint.2016.04.015, 2016.
- 716 Tuet, W. Y., Fok, S., Verma, V., Rodriguez, M. S. T., Grosberg, A., Champion, J. A., and Ng, N. L.: Dose-  
 717 dependent intracellular reactive oxygen and nitrogen species (ROS/RNS) production from particulate matter  
 718 exposure: comparison to oxidative potential and chemical composition, *Atmospheric Environment*, 144, 335-344,  
 719 2016.
- 720 Verma, V., Rico-Martinez, R., Kotra, N., King, L., Liu, J., Snell, T. W., and Weber, R. J.: Contribution of water-  
 721 soluble and insoluble components and their hydrophobic/hydrophilic subfractions to the reactive oxygen species-  
 722 generating potential of fine ambient aerosols, *Environmental Science & Technology*, 46, 11384-11392,  
 723 10.1021/es302484r, 2012.
- 724 Verma, V., Fang, T., Guo, H., King, L., Bates, J., Peltier, R., Edgerton, E., Russell, A., and Weber, R.: Reactive  
 725 oxygen species associated with water-soluble PM<sub>2.5</sub> in the southeastern United States: spatiotemporal trends and  
 726 source apportionment, *Atmospheric Chemistry and Physics*, 14, 12915-12930, 2014.
- 727 Vidrio, E., Phuah, C. H., Dillner, A. M., and Anastasio, C.: Generation of hydroxyl radicals from ambient fine  
 728 particles in a surrogate lung fluid solution, *Environmental Science & Technology*, 43, 922-927, 10.1021/es801653u,  
 729 2009.



- 730 Visentin, M., Pagnoni, A., Sarti, E., and Pietrogrande, M. C.: Urban PM<sub>2.5</sub> oxidative potential: Importance of  
 731 chemical species and comparison of two spectrophotometric cell-free assays, *Environmental Pollution*, 219, 72-79,  
 732 10.1016/j.envpol.2016.09.047, 2016.
- 733 Wang, Y., Plewa, M. J., Mukherjee, U. K., and Verma, V.: Assessing the cytotoxicity of ambient particulate matter  
 734 (PM) using Chinese hamster ovary (CHO) cells and its relationship with the PM chemical composition and  
 735 oxidative potential, *Atmospheric Environment*, 179, 132-141, 10.1016/j.atmosenv.2018.02.025, 2018.
- 736 Wei, J., Yu, H., Wang, Y., and Verma, V.: Complexation of iron and copper in ambient particulate matter and its  
 737 effect on the oxidative potential measured in a surrogate lung fluid, *Environmental Science & Technology*, 53, 1661-  
 738 1671, 2018.
- 739 Weichenthal, S., Lavigne, E., Evans, G., Pollitt, K., and Burnett, R. T.: Ambient PM<sub>2.5</sub> and risk of emergency room  
 740 visits for myocardial infarction: impact of regional PM<sub>2.5</sub> oxidative potential: a case-crossover study, *Environmental*  
 741 *Health*, 15, 46, 10.1186/s12940-016-0129-9, 2016a.
- 742 Weichenthal, S., Shekarzifard, M., Traub, A., Kulka, R., Al-Rijleh, K., Anowar, S., Evans, G., and Hatzopoulou,  
 743 M.: Within-city spatial variations in multiple measures of PM<sub>2.5</sub> oxidative potential in Toronto, Canada,  
 744 *Environmental Science & Technology*, 53, 2799-2810, 2019.
- 745 Weichenthal, S. A., Lavigne, E., Evans, G. J., Godri Pollitt, K. J., and Burnett, R. T.: Fine particulate matter and  
 746 emergency room visits for respiratory illness. Effect modification by oxidative potential, *American Journal of*  
 747 *Respiratory and Critical Care Medicine*, 194, 577-586, 2016b.
- 748 Wessels, A., Birmili, W., Albrecht, C., Hellack, B., Jermann, E., Wick, G., Harrison, R. M., and Schins, R. P.:  
 749 Oxidant generation and toxicity of size-fractionated ambient particles in human lung epithelial cells, *Environmental*  
 750 *Science & Technology*, 44, 3539-3545, 2010.
- 751 Xiang, S., Yu, Y. T., Hu, Z., and Noll, K. E.: Characterization of dispersion and ultrafine-particle emission factors  
 752 based on near-roadway monitoring Part II: Heavy duty vehicles, *Aerosol and Air Quality Research*, 19, 2421-2431,  
 753 2019.
- 754 Xing, Y.-F., Xu, Y.-H., Shi, M.-H., and Lian, Y.-X.: The impact of PM<sub>2.5</sub> on the human respiratory system, *Journal*  
 755 *of Thoracic Disease*, 8, E69-E74, 2016.
- 756 Xiong, Q., Yu, H., Wang, R., Wei, J., and Verma, V.: Rethinking the dithiothreitol-based particulate matter  
 757 oxidative potential: measuring dithiothreitol consumption versus reactive oxygen species generation, *Environmental*  
 758 *Science & Technology*, 51, 6507-6514, 10.1021/acs.est.7b01272, 2017.
- 759 Xu, Z., Xu, X., Zhong, M., Hotchkiss, I. P., Lewandowski, R. P., Wagner, J. G., Bramble, L. A., Yang, Y., Wang,  
 760 A., and Harkema, J. R.: Ambient particulate air pollution induces oxidative stress and alterations of mitochondria  
 761 and gene expression in brown and white adipose tissues, *Particle and Fibre Toxicology*, 8, 1-14, 2011.
- 762 Yan, Z., Wang, J., Li, J., Jiang, N., Zhang, R., Yang, W., Yao, W., and Wu, W.: Oxidative stress and endocytosis are  
 763 involved in upregulation of interleukin-8 expression in airway cells exposed to PM<sub>2.5</sub>, *Environmental Toxicology*,  
 764 31, 1869-1878, 10.1002/tox.22188, 2016.





- 765 Yang, A., Jedynska, A., Hellack, B., Kooter, I., Hoek, G., Brunekreef, B., Kuhlbusch, T. A., Cassee, F. R., and  
 766 Janssen, N. A.: Measurement of the oxidative potential of PM<sub>2.5</sub> and its constituents: The effect of extraction solvent  
 767 and filter type, *Atmospheric Environment*, 83, 35–42, 10.1016/j.atmosenv.2013.10.049, 2014.
- 768 Yang, A., Hellack, B., Leseman, D., Brunekreef, B., Kuhlbusch, T. A., Cassee, F. R., Hoek, G., and Janssen, N. A.:  
 769 Temporal and spatial variation of the metal-related oxidative potential of PM<sub>2.5</sub> and its relation to PM<sub>2.5</sub> mass and  
 770 elemental composition, *Atmospheric Environment*, 102, 62–69, 2015a.
- 771 Yang, A., Wang, M., Eeftens, M., Beelen, R., Dons, E., Leseman, D. L., Brunekreef, B., Cassee, F. R., Janssen, N.  
 772 A., and Hoek, G.: Spatial variation and land use regression modeling of the oxidative potential of fine particles,  
 773 *Environmental Health Perspectives*, 123, 1187–1192, 2015b.
- 774 Yang, A., Janssen, N. A., Brunekreef, B., Cassee, F. R., Hoek, G., and Gehring, U.: Children's respiratory health and  
 775 oxidative potential of PM<sub>2.5</sub>: the PIAMA birth cohort study, *Occupational & Environmental Medicine*, 73, 154–160,  
 776 10.1136/oemed-2015-103175, 2016.
- 777 Yu, H., Wei, J., Cheng, Y., Subedi, K., and Verma, V.: Synergistic and antagonistic interactions among the  
 778 particulate matter components in generating reactive oxygen species based on the dithiothreitol assay,  
 779 *Environmental Science & Technology*, 52, 2261–2270, 10.1021/acs.est.7b04261, 2018.
- 780 Yu, H., Puthussery, J. V., and Verma, V.: A semi-automated multi-endpoint reactive oxygen species activity  
 781 analyzer (SAMERA) for measuring the oxidative potential of ambient PM<sub>2.5</sub> aqueous extracts, *Aerosol Science and*  
 782 *Technology*, 54, 304–320, 2020.
- 783 Yu, S., Liu, W., Xu, Y., Yi, K., Zhou, M., Tao, S., and Liu, W.: Characteristics and oxidative potential of  
 784 atmospheric PM<sub>2.5</sub> in Beijing: Source apportionment and seasonal variation, *Science of the Total Environment*, 650,  
 785 277–287, 2019.
- 786 Zhang, Y., Schauer, J. J., Shafer, M. M., Hannigan, M. P., and Dutton, S. J.: Source apportionment of *in vitro*  
 787 reactive oxygen species bioassay activity from atmospheric particulate matter, *Environmental Science &*  
 788 *Technology*, 42, 7502–7509, 10.1021/es800126y, 2008.
- 789 Zhou, J., Ito, K., Lall, R., Lippmann, M., and Thurston, G.: Time-series analysis of mortality effects of fine  
 790 particulate matter components in Detroit and Seattle, *Environmental Health Perspectives*, 119, 461–466, 2011.
- 791 Zuo, L., Otenbaker, N. P., Rose, B. A., and Salisbury, K. S.: Molecular mechanisms of reactive oxygen species-  
 792 related pulmonary inflammation and asthma, *Molecular Immunology*, 56, 57–63,  
 793 https://doi.org/10.1016/j.molimm.2013.04.002, 2013.





## 794 Figures and Tables

795 **Table 1.** Average and standard deviation of OP from various control groups (N = 10) analyzed by SAMERA.

Endpoint	Unit	Negative control		Chemical used as positive control	Positive control		Coefficient of variation (CoV, %)
		Average	Standard deviation		Average	Standard deviation	
OP <sup>AA</sup>	μM/min	0.18	0.07	1 μM Cu	0.34	0.04	11.8
OP <sup>GSH</sup>	μM/min	0.26	0.06	1 μM Cu	0.77	0.02	2.6
OP <sup>OH-SLF</sup>	nM/min	7.69	1.37	2 μM Fe	13.80	0.70	5.1
OP <sup>DTT</sup>	μM/min	0.48	0.07	0.2 μM PQ	1.84	0.02	1.1
OP <sup>OH-DTT</sup>	nM/min	0.55	0.07	0.2 μM 5-H-1,4-NQ	15.45	1.19	7.7

796 **Table 2.** Seasonal averages ( $\pm$  standard deviation) of PM<sub>2.5</sub> mass concentrations (unit: μg/m<sup>3</sup>) at our sampling sites.

	CHI	STL	IND	CMP	BON
Summer 2018	11.2 $\pm$ 3.2	14.7 $\pm$ 3.4	11.9 $\pm$ 3.5	11.4 $\pm$ 3.9	10.4 $\pm$ 2.0
Fall 2018	10.9 $\pm$ 3.4	13.1 $\pm$ 3.7	11.5 $\pm$ 4.2	7.5 $\pm$ 4.3	9.7 $\pm$ 3.5
Winter 2018	14.6 $\pm$ 3.6	11.8 $\pm$ 2.8	11.0 $\pm$ 2.7	10.0 $\pm$ 3.0	8.6 $\pm$ 3.0
Spring 2019	12.6 $\pm$ 4.2	13.8 $\pm$ 4.0	12.2 $\pm$ 2.1	11.6 $\pm$ 3.1	9.2 $\pm$ 2.3

797 **Table 3.** Pearson's correlation coefficient (r) and the associated levels of significance (P) between water-soluble and  
 798 methanol-soluble OPv for different endpoints at five sampling sites. Correlations with  $r > 0.60$  are shown in **bold**.

Site	Pearson's r/significance level (P) for OP endpoints				
	OP <sup>AA</sup>	OP <sup>GSH</sup>	OP <sup>OH-SLF</sup>	OP <sup>DTT</sup>	OP <sup>OH-DTT</sup>
CHI	0.09/0.55	0.34/0.03	0.53/<0.01	0.55/<0.01	0.40/<0.01
STL	0.24/0.10	0.11/0.48	0.18/0.24	0.28/0.11	0.38/<0.01
IND	0.24/0.08	0.40/<0.01	0.33/0.02	0.43/<0.01	0.21/0.14
CMP	0.42/<0.01	<b>0.63/&lt;0.01</b>	0.10/0.51	<b>0.74/&lt;0.01</b>	0.58/<0.01
BON	0.60/<0.01	0.52/<0.01	0.41/<0.01	<b>0.68/&lt;0.01</b>	0.54/<0.01

799 **Table 4.** Pearson's r, the associated levels of significance (P) and slope for simple linear regression of water-soluble  
 800 OPv versus PM<sub>2.5</sub> mass concentration at five sampling sites. Correlations with  $r > 0.60$  are shown in **bold**. All slope  
 801 values are in *italic*.

### 802 (a) Water-soluble OP

		CHI	STL	IND	CMP	BON
OP <sup>AA</sup>	Pearson's r/P	-0.02/0.89	0.33/0.02	0.19/0.18	0.54/<0.01	0.26/0.09
	<i>Slope (nmol/min/μg)</i>	<i>0.000</i>	<i>0.005</i>	<i>0.004</i>	<i>0.031</i>	<i>0.007</i>
OP <sup>GSH</sup>	Pearson's r/P	0.45/<0.01	0.34/0.02	0.45/<0.01	<b>0.72/&lt;0.01</b>	0.38/0.01
	<i>Slope (nmol/min/μg)</i>	<i>0.005</i>	<i>0.003</i>	<i>0.005</i>	<i>0.016</i>	<i>0.005</i>
OP <sup>OH-SLF</sup>	Pearson's r/P	0.09/0.55	0.26/0.08	0.37/<0.01	0.43/<0.01	0.24/0.12
	<i>Slope (pmol/min/μg)</i>	<i>0.041</i>	<i>0.107</i>	<i>0.128</i>	<i>0.277</i>	<i>0.165</i>
OP <sup>DTT</sup>	Pearson's r/P	<b>0.62/&lt;0.01</b>	0.27/0.07	0.55/<0.01	<b>0.82/&lt;0.01</b>	<b>0.63/&lt;0.01</b>
	<i>Slope (nmol/min/μg)</i>	<i>0.013</i>	<i>0.005</i>	<i>0.013</i>	<i>0.020</i>	<i>0.015</i>
OP <sup>OH-DTT</sup>	Pearson's r/P	0.24/0.12	0.60/<0.01	0.37/<0.01	0.51/<0.01	0.45/<0.01
	<i>Slope (pmol/min/μg)</i>	<i>0.043</i>	<i>0.062</i>	<i>0.051</i>	<i>0.048</i>	<i>0.052</i>

803



(b) Methanol-soluble OP

		CHI	STL	IND	CMP	BON
OP <sup>AA</sup>	Pearson's r/P	0.55/<0.01	0.12/0.43	0.52/<0.01	<b>0.64/&lt;0.01</b>	<b>0.61/&lt;0.01</b>
	<i>Slope (nmol/min/μg)</i>	0.010	0.002	0.010	0.011	0.012
OP <sup>GSH</sup>	Pearson's r/P	0.53/<0.01	0.38/<0.01	0.51/<0.01	<b>0.73/&lt;0.01</b>	<b>0.63/&lt;0.01</b>
	<i>Slope (nmol/min/μg)</i>	0.007	0.005	0.007	0.012	0.009
OP <sup>OH-SLF</sup>	Pearson's r/P	0.19/0.23	0.34/0.02	0.45/<0.01	0.48/<0.01	0.52/<0.01
	<i>Slope (pmol/min/μg)</i>	0.264	0.514	0.666	0.576	0.735
OP <sup>DTT</sup>	Pearson's r/P	0.54/<0.01	0.49/<0.01	<b>0.61/&lt;0.01</b>	<b>0.79/&lt;0.01</b>	<b>0.61/&lt;0.01</b>
	<i>Slope (nmol/min/μg)</i>	0.017	0.016	0.019	0.028	0.022
OP <sup>OH-DTT</sup>	Pearson's r/P	0.25/0.10	0.44/0.02	0.51/<0.01	0.43/<0.01	0.50/<0.01
	<i>Slope (pmol/min/μg)</i>	0.072	0.079	0.143	0.075	0.165

**Table 5.** Pearson's correlation coefficient (r) and the associated level of significance (P) among various endpoints of OPv measured at five sampling sites. The values below the diagonal are for water-soluble OPv, while above are for methanol-soluble OPv. Correlations with  $r > 0.60$  are shown in **bold**.

(a) CHI

OP endpoint	OP <sup>AA</sup>	Pearson's r/significance level (P) for OP endpoints			
		OP <sup>GSH</sup>	OP <sup>OH-SLF</sup>	OP <sup>DTT</sup>	OP <sup>OH-DTT</sup>
OP <sup>AA</sup>		<b>0.66/&lt;0.01</b>	0.60/<0.01	<b>0.69/&lt;0.01</b>	0.49/<0.01
OP <sup>GSH</sup>	0.32/0.04		0.30/0.05	0.45/<0.01	0.17/0.27
OP <sup>OH-SLF</sup>	0.09/0.58	0.39/<0.01		0.53/<0.01	<b>0.82/&lt;0.01</b>
OP <sup>DTT</sup>	0.05/0.73	0.40/<0.01	0.40/<0.01		<b>0.64/&lt;0.01</b>
OP <sup>OH-DTT</sup>	0.03/0.86	0.30/0.05	0.48/<0.01	0.18/0.24	
	OP <sup>AA</sup>	OP <sup>GSH</sup>	OP <sup>OH-SLF</sup>	OP <sup>DTT</sup>	OP <sup>OH-DTT</sup>

(b) STL

OP endpoint	OP <sup>AA</sup>	Pearson's r/significance level (P) for OP endpoints			
		OP <sup>GSH</sup>	OP <sup>OH-SLF</sup>	OP <sup>DTT</sup>	OP <sup>OH-DTT</sup>
OP <sup>AA</sup>		0.40/<0.01	0.19/0.20	0.50/<0.01	0.33/0.02
OP <sup>GSH</sup>	0.30/0.05		0.13/0.40	0.36/0.01	0.23/0.12
OP <sup>OH-SLF</sup>	0.51/<0.01	0.17/0.26		0.17/0.26	0.42/<0.01
OP <sup>DTT</sup>	0.28/0.06	0.29/0.05	0.22/0.14		0.57/<0.01
OP <sup>OH-DTT</sup>	0.40/<0.01	0.38/<0.01	0.53/<0.01	0.34/0.02	
	OP <sup>AA</sup>	OP <sup>GSH</sup>	OP <sup>OH-SLF</sup>	OP <sup>DTT</sup>	OP <sup>OH-DTT</sup>

(c) IND

OP endpoint	OP <sup>AA</sup>	Pearson's r/significance level (P) for OP endpoints			
		OP <sup>GSH</sup>	OP <sup>OH-SLF</sup>	OP <sup>DTT</sup>	OP <sup>OH-DTT</sup>
OP <sup>AA</sup>		0.57/<0.01	0.54/<0.01	<b>0.62/&lt;0.01</b>	0.57/<0.01
OP <sup>GSH</sup>	0.37/<0.01		0.59/<0.01	0.52/<0.01	0.55/<0.01
OP <sup>OH-SLF</sup>	0.32/0.02	0.23/0.10		0.44/<0.01	<b>0.84/&lt;0.01</b>
OP <sup>DTT</sup>	0.17/0.22	0.42/<0.01	0.44/<0.01		0.54/<0.01
OP <sup>OH-DTT</sup>	0.08/0.58	0.20/0.14	0.29/0.03	0.15/0.29	
	OP <sup>AA</sup>	OP <sup>GSH</sup>	OP <sup>OH-SLF</sup>	OP <sup>DTT</sup>	OP <sup>OH-DTT</sup>



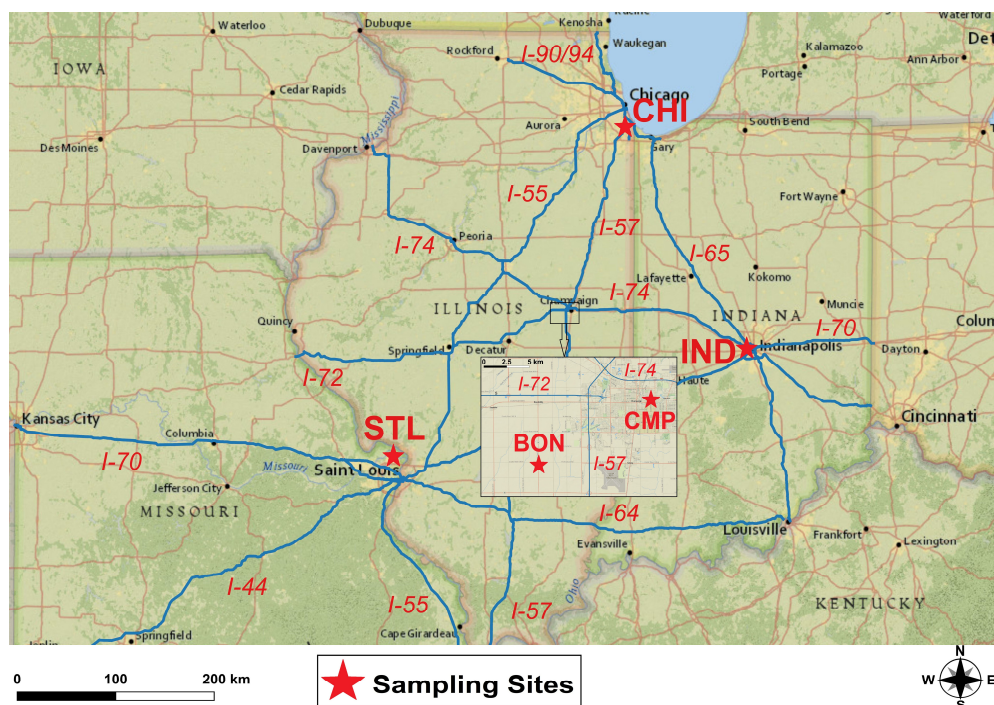
812 (d) CMP

OP endpoint	Pearson's r/significance level (P) for OP endpoints				
	OP <sup>AA</sup>	OP <sup>GSH</sup>	OP <sup>OH-SLF</sup>	OP <sup>DTT</sup>	OP <sup>OH-DTT</sup>
OP <sup>AA</sup>		0.55/<0.01	0.46/<0.01	<b>0.70/&lt;0.01</b>	0.45/<0.01
OP <sup>GSH</sup>	<b>0.68/&lt;0.01</b>		0.30/0.04	<b>0.69/&lt;0.01</b>	0.15/0.32
OP <sup>OH-SLF</sup>	<b>0.77/&lt;0.01</b>	<b>0.80/&lt;0.01</b>		0.37/<0.01	<b>0.66/&lt;0.01</b>
OP <sup>DTT</sup>	<b>0.80/&lt;0.01</b>	<b>0.73/&lt;0.01</b>	0.58/<0.01		0.35/0.01
OP <sup>OH-DTT</sup>	0.02/0.91	0.26/0.07	0.15/0.31	0.29/0.04	
	OP <sup>AA</sup>	OP <sup>GSH</sup>	OP <sup>OH-SLF</sup>	OP <sup>DTT</sup>	OP <sup>OH-DTT</sup>

813 (e) BON

OP endpoint	Pearson's r/significance level (P) for OP endpoints				
	OP <sup>AA</sup>	OP <sup>GSH</sup>	OP <sup>OH-SLF</sup>	OP <sup>DTT</sup>	OP <sup>OH-DTT</sup>
OP <sup>AA</sup>		<b>0.66/&lt;0.01</b>	<b>0.77/&lt;0.01</b>	<b>0.70/&lt;0.01</b>	<b>0.61/&lt;0.01</b>
OP <sup>GSH</sup>	<b>0.85/&lt;0.01</b>		<b>0.68/&lt;0.01</b>	0.60/<0.01	0.53/<0.01
OP <sup>OH-SLF</sup>	0.57/<0.01	<b>0.64/&lt;0.01</b>		<b>0.69/&lt;0.01</b>	<b>0.78/&lt;0.01</b>
OP <sup>DTT</sup>	0.51/<0.01	0.57/<0.01	0.30/0.05		<b>0.68/&lt;0.01</b>
OP <sup>OH-DTT</sup>	0.19/0.21	0.31/0.04	0.28/0.06	0.32/0.03	
	OP <sup>AA</sup>	OP <sup>GSH</sup>	OP <sup>OH-SLF</sup>	OP <sup>DTT</sup>	OP <sup>OH-DTT</sup>

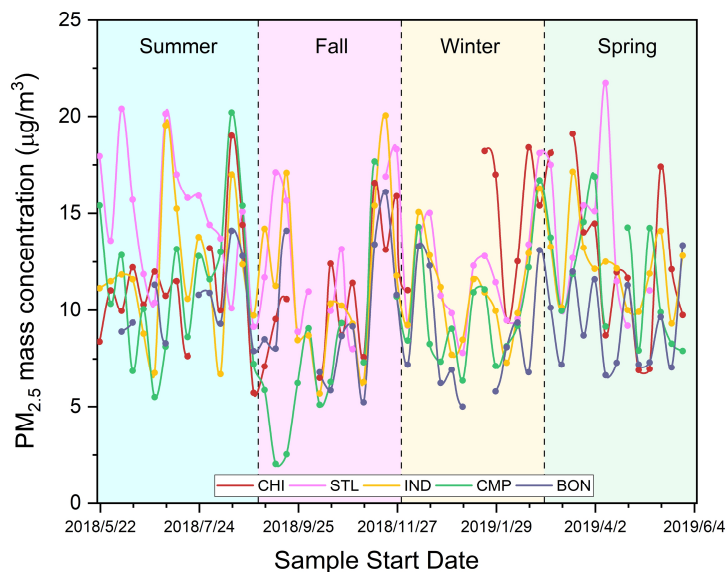
814



815

816

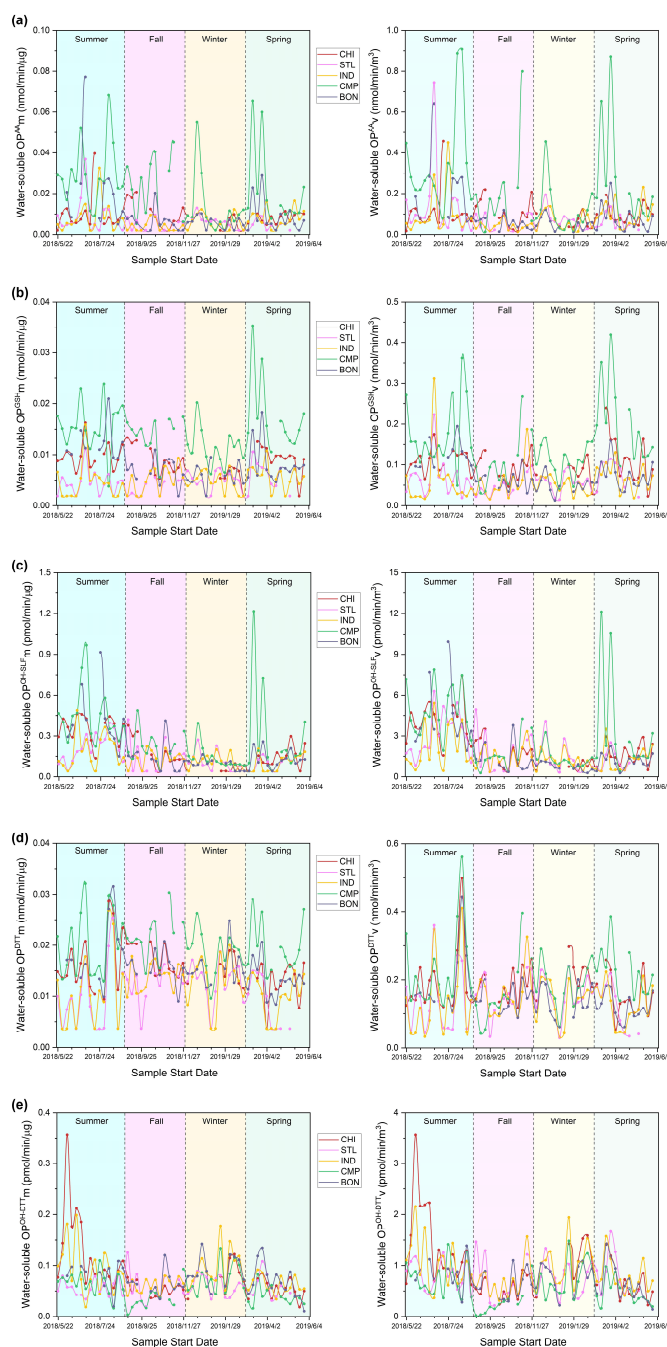
**Figure 1.** Map for our five sampling sites in the Midwest US.



817

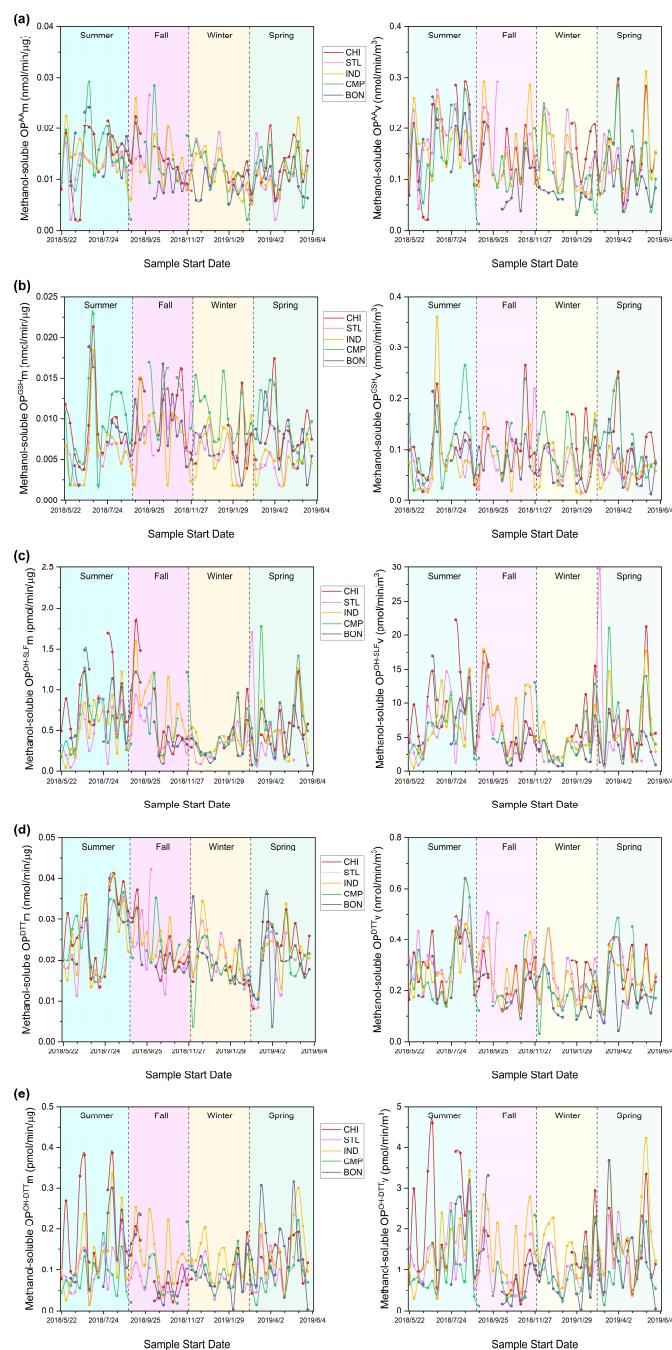
818

**Figure 2.** Time series of  $PM_{2.5}$  mass concentrations at our sampling sites in the Midwest US.



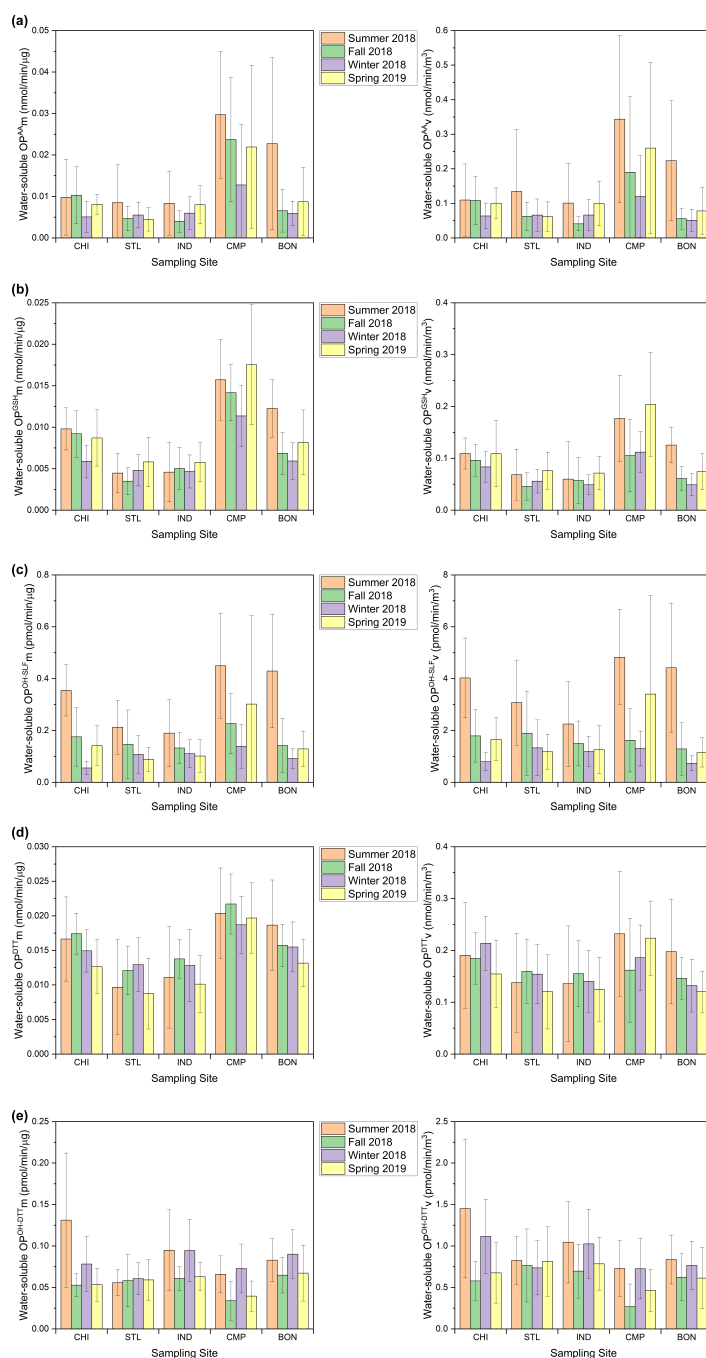
819

820 **Figure 3.** Time series of mass-(left) and volume-(right) normalized water-soluble OP activities for (a)  
 821  $OP^{AA}$ , (b)  $OP^{GSH}$ , (c)  $OP^{OH-SLF}$ , (d)  $OP^{DTT}$  and (e)  $OP^{OH-DTT}$  at our sampling sites.



822

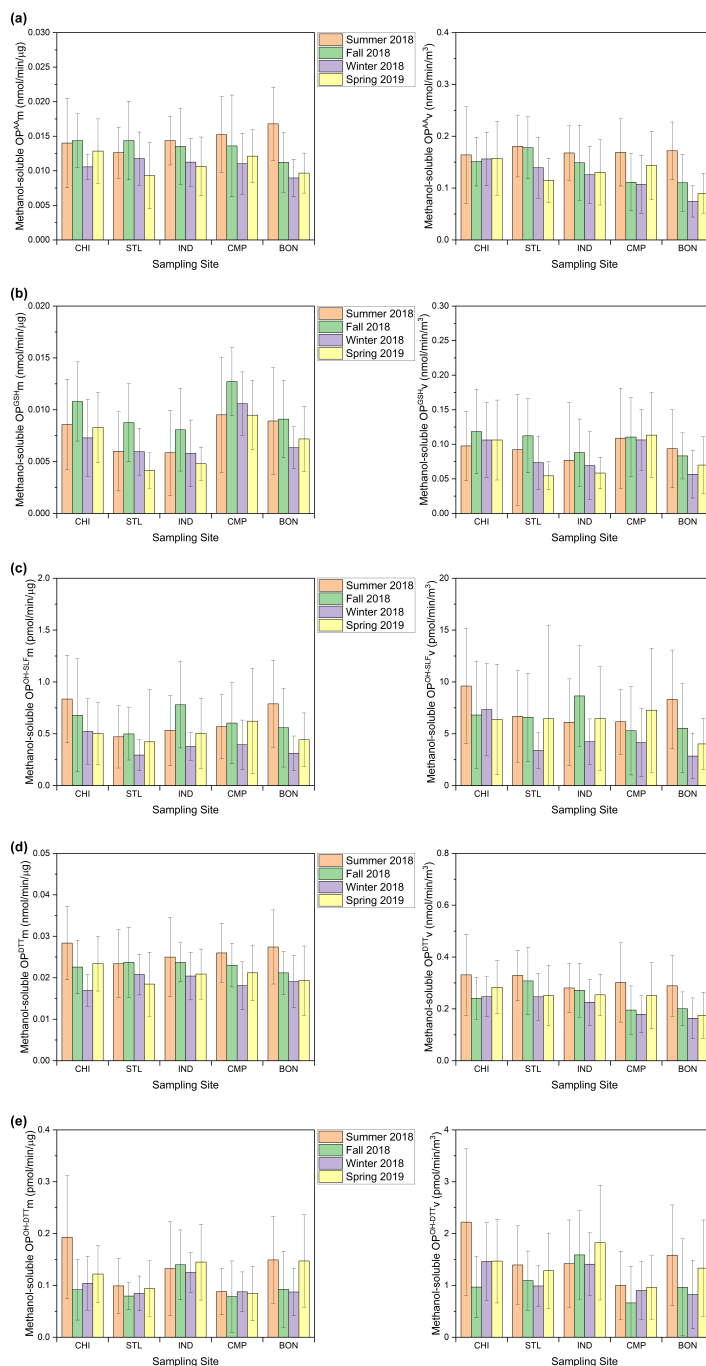
823 **Figure 4.** Time series of mass-(left) and volume-(right) normalized methanol-soluble OP activities for (a)  
 824 OP<sup>AA</sup>, (b) OP<sup>GSH</sup>, (c) OP<sup>OH-SLF</sup>, (d) OP<sup>DTT</sup> and (e) OP<sup>OH-DTT</sup> at our sampling sites.



825

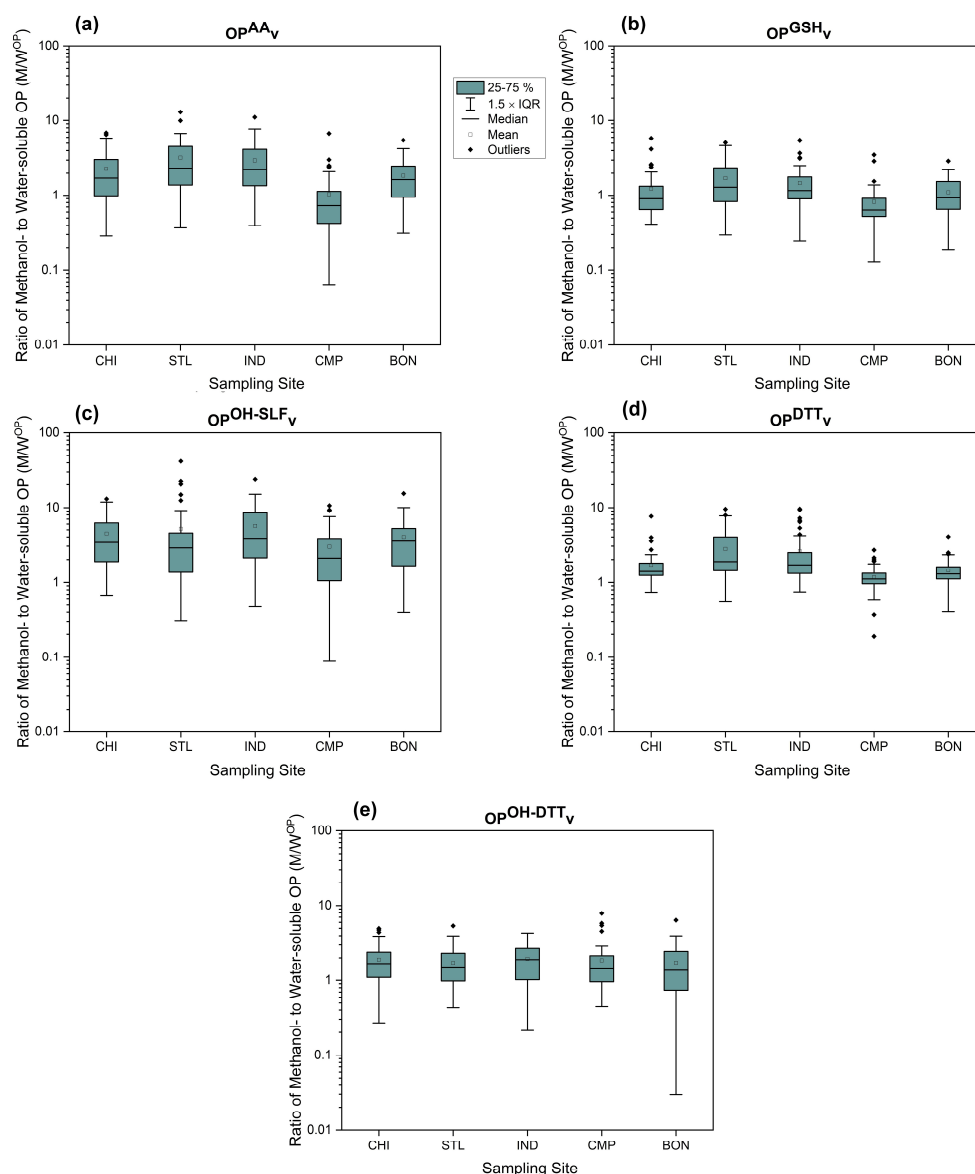
826 **Figure 5.** Seasonal averages of mass-(left) and volume-(right) normalized water-soluble OP activities for  
 827 (a)  $OP^{AA}$ , (b)  $OP^{GSH}$ , (c)  $OP^{OH-SLF}$ , (d)  $OP^{DTT}$  and (e)  $OP^{OH-DTT}$  at our sampling sites.





828

829 **Figure 6.** Seasonal averages of mass-(left) and volume-(right) normalized methanol-soluble OP activities  
 830 for (a)  $OP^{AA}$ , (b)  $OP^{GSH}$ , (c)  $OP^{OH-SLF}$ , (d)  $OP^{DTT}$  and (e)  $OP^{OH-DTT}$  at our sampling sites.



831

832 **Figure 7.** Ratio of methanol-soluble OP<sub>v</sub> to water-soluble OP<sub>v</sub> (M/W<sup>OP</sup>) for (a) OP<sup>AA</sup><sub>v</sub>, (b) OP<sup>GSH</sup><sub>v</sub>, (c)  
 833 OP<sup>OH-SLF</sup><sub>v</sub>, (d) OP<sup>DTT</sup><sub>v</sub>, and (e) OP<sup>OH-DTT</sup><sub>v</sub> at five sampling sites.

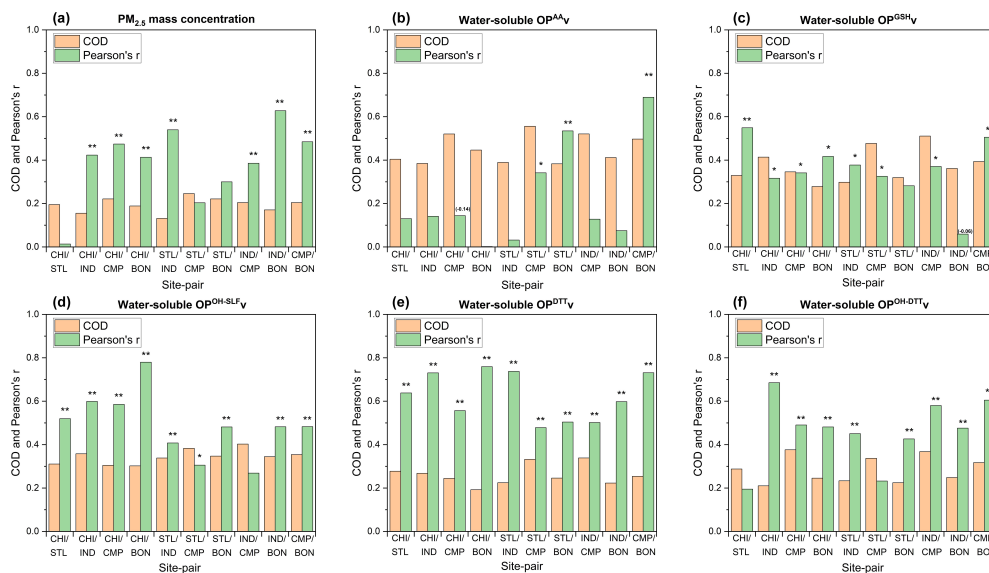


**Figure 8.** Coefficient of divergence (CoD) and Pearson's  $r$  for site-to-site comparison of (a)  $\text{PM}_{2.5}$  mass and water-soluble OP activities: (b)  $\text{OP}^{\text{AA}}_{\text{v}}$ , (c)  $\text{OP}^{\text{GSH}}_{\text{v}}$ , (d)  $\text{OP}^{\text{OH-SLF}}_{\text{v}}$ , (e)  $\text{OP}^{\text{DTT}}_{\text{v}}$  and (f)  $\text{OP}^{\text{OH-DTT}}_{\text{v}}$ . Asterisks - \* and \*\* on the bars of Pearson's  $r$  indicate significant ( $P < 0.05$ ) and very significant ( $P < 0.01$ ) correlations, respectively. Note:  $r$  for the correlations of  $\text{OP}^{\text{AA}}_{\text{v}}$  between CHI and CMP and for the correlations of  $\text{OP}^{\text{GSH}}_{\text{v}}$  between IND and BON were negative (-0.14 and -0.06, respectively).

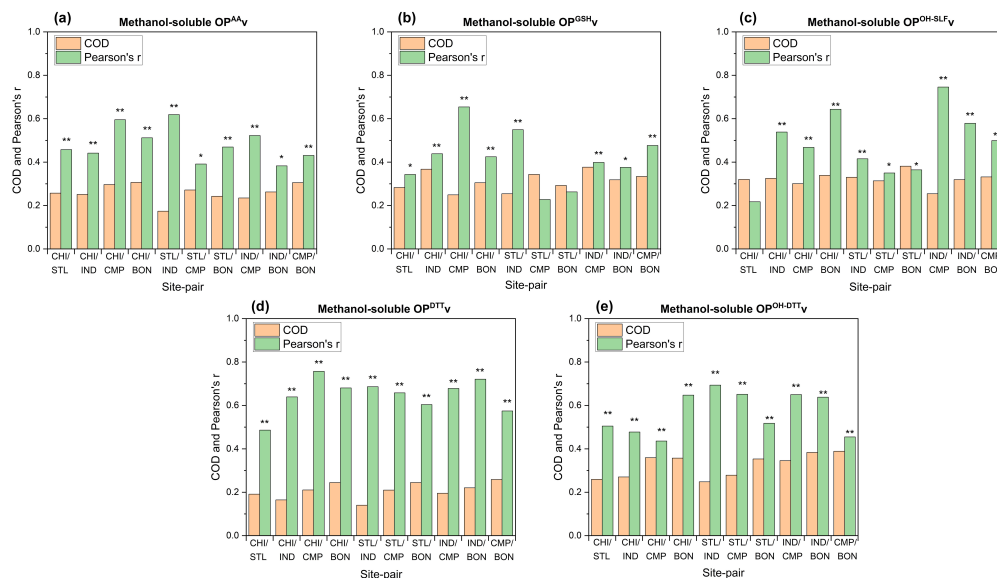


**Figure 9.** Coefficient of divergence (CoD) and Pearson's  $r$  for site-to-site comparison of methanol-soluble OP activities: (a)  $\text{OP}^{\text{AA}}_{\text{v}}$ , (b)  $\text{OP}^{\text{GSH}}_{\text{v}}$ , (c)  $\text{OP}^{\text{OH-SLF}}_{\text{v}}$ , (d)  $\text{OP}^{\text{DTT}}_{\text{v}}$  and (e)  $\text{OP}^{\text{OH-DTT}}_{\text{v}}$ . Asterisks - \* and \*\* on the bars of Pearson's  $r$  indicate significant ( $P < 0.05$ ) and very significant ( $P < 0.01$ ) correlations, respectively.